We thank the patients and family members for their participation; M. Tsuchiya, Y. Hazama, Y. Koike, R. Izumita, and M. Nihonmatsu for technical assistance; and Drs. B. Vogelstein (Howard Hughes Medical Institute and Sidney Kimmel Comprehensive Cancer Center), T. Katagiri (Saitama Medical School Research Center for Genomic Medicine), and E. Schwartz (Institut für Biotechnologie, Martin Luther Universität Halle–Wittenberg) for their generous gifts of plasmids.

REFERENCES

1. Chui HC. Subcortical ischemic vascular dementia. Neurol Clin 2007;25:717-40.
2. Joutel A, Corpechot C, Ducros A, et al. Notch3 mutations in CADASIL, a hereditary adult-onset condition causing stroke and dementia. Nature 1996;383:707-10.
3. Richards A, van den Maagdenberg AM, Jen JC, et al. C-terminal truncations in human 3′-5′ DNA exonuclease TREX1 cause autosomal dominant retinal vasculopathy with cerebral leukodystrophy. Nat Genet 2007;39:1068-70.
4. Gould DB, Phalan FC, van Mil SE, et al. Role of COL4A1 in small-vessel disease and hemorrhagic stroke. N Engl J Med 2006;354:1489-96.
5. Revesz T, Ghiso J, Lashley T, et al. Cerebral amyloid angiopathies: a pathologic, biochemical, and genetic view. J Neuropathol Exp Neurol 2003;62:885-98.
6. Fukutake T, Hirayama K. Familial young-adult-onset arteriosclerotic leukoencephalopathy with alopecia and lumbago without arterial hypertension. Eur Neurol 1995;35:69-79.
7. Maeda S, Nakayama H, Isaka K, Aihara Y, Nemoto S. Familial unusual encephalopathy of Binswanger's type without hypertension. Folia Psychiatr Neurol Jpn 1976;30:165-77.
8. Yanagawa S, Ito N, Arima K, Ikeda S. Cerebral autosomal recessive arteriopathy with subcortical infarcts and leukoencephalopathy. Neurology 2002;58:817-20.
9. Oide T, Nakayama H, Yanagawa S, Ito N, Ikeda S, Arima K. Extensive loss of arterial medial smooth muscle cells and mural extracellular matrix in cerebral autosomal recessive arteriopathy with subcortical infarcts and leukoencephalopathy (CARASIL). Neuropathology 2008;28:132-42.
10. Okeda R, Murayama S, Sawabe M, Kuroiwa T. Pathology of the cerebral artery in Binswanger's disease in the aged: observation by serial sections and morphometry of the cerebral arteries. Neuropathology 2004;24:21-9.
11. Tanoi Y, Okeda R, Budka H. Binswanger's encephalopathy: serial sections and morphometry of the cerebral arteries. Acta Neuropathol 2000;100:347-55.
12. Lathrop GM, Lalouel JM, Julier C, Ott J. Strategies for multilocus linkage analysis in humans. Proc Natl Acad Sci U S A 1984; 81:3443-6.
13. Cottingham RW Jr, Idury RM, Schäffer AA. Faster sequential genetic linkage computations. Am J Hum Genet 1993;53:252-63.
14. Hu SI, Carozza M, Klein M, Nantermet P, Luk D, Crowl RM. Human HtrA, an evolutionarily conserved serine protease identified as a differentially expressed gene product in osteoarthritic cartilage. J Biol Chem 1998;273:34406-12.
15. Brunner AM, Marquardt H, Malacko AR, Lioubin MN, Purchio AF. Site-directed mutagenesis of cysteine residues in the pro region of the transforming growth factor β 1 precursor: expression and characterization of mutant proteins. J Biol Chem 1989;264:13660-4.
16. Oka C, Tsujimoto R, Kajikawa M, et al. HtrA1 serine protease inhibits signaling mediated by Tgfβ family proteins. Development 2004;131:1041-53.
17. Katagiri T, Imada M, Yanai T, Suda T, Takahashi N, Kamijo R. Identification of a BMP-responsive element in Id1, the gene for inhibition of myogenesis. Genes Cells 2002;7:949-60.
18. Hillger F, Herr G, Rudolph R, Schwarz E. Biophysical comparison of BMP-2, ProBMP-2, and the free pro-peptide reveals stabilization of the pro-peptide by the mature growth factor. J Biol Chem 2005;280:14974-80.
19. De Luca A, De Falco M, Severino A, et al. Distribution of the serine protease HtrA1 in normal human tissues. J Histochem Cytochem 2003;51:1279-84.
20. Kuzmiak HA, Maquat LE. Applying nonsense-mediated mRNA decay research to the clinic: progress and challenges. Trends Mol Med 2006;12:306-16.
21. Gazzerro E, Gangji V, Canalis E. Bone morphogenetic proteins induce the expression of noggin, which limits their activity in cultured rat osteoblasts. J Clin Invest 1998;102:2106-14.
22. Glukhova MA, Frid MG, Shekhonin BV, et al. Expression of extra domain A fibronectin sequence in vascular smooth muscle cells is phenotype dependent. J Cell Biol 1989;109:357-66.
23. Leask A, Abraham DJ. TGF-β signaling and the fibrotic response. FASEB J 2004;18:816-27.
24. Schönherr E, Järveläinen HT, Sandell LJ, Wight TN. Effects of platelet-derived growth factor and transforming growth factor-β 1 on the synthesis of a large versican-like chondroitin sulfate proteoglycan by arterial smooth muscle cells. J Biol Chem 1991;266:17640-7.
25. Grainger DJ. Transforming growth factor β and atherosclerosis: so far, so good for the protective cytokine hypothesis. Arterioscler Thromb Vasc Biol 2004; 24:399-404.
26. ten Dijke P, Arthur HM. Extracellular control of TGFβ signalling in vascular development and disease. Nat Rev Mol Cell Biol 2007;8:857-69.
27. O'Callaghan CJ, Williams B. Mechanical strain-induced extracellular matrix production by human vascular smooth muscle cells: role of TGF-β(1). Hypertension 2000;36:319-24.
28. Liu X, Alexander V, Vijayachandra K, Bhogte E, Diamond I, Glick A. Conditional epidermal expression of TGFβ 1 blocks neonatal lethality but causes a reversible hyperplasia and alopecia. Proc Natl Acad Sci U S A 2001;98:9139-44.
29. Botchkarev VA. Bone morphogenetic proteins and their antagonists in skin and hair follicle biology. J Invest Dermatol 2003;120:36-47.
30. Yoon BS, Lyons KM. Multiple functions of BMPs in chondrogenesis. J Cell Biochem 2004;93:93-103.
31. Hadfield KD, Rock CF, Inkson CA, et al. HtrA1 inhibits mineral deposition by osteoblasts: requirement for the protease and PDZ domains. J Biol Chem 2008;283: 5928-38.
32. Clausen T, Southan C, Ehrmann M. The HtrA family of proteases: implications for protein composition and cell fate. Mol Cell 2002;10:443-55.
33. Tsuchiya A, Yano M, Tocharus J, et al. Expression of mouse HtrA1 serine protease in normal bone and cartilage and its upregulation in joint cartilage damaged by experimental arthritis. Bone 2005;37:323-36.
34. Grau S, Baldi A, Bussani R, et al. Implications of the serine protease HtrA1 in amyloid precursor protein processing. Proc Natl Acad Sci U S A 2005;102:6021-6.
35. Gilicze A, Kohalmi B, Pocza P, et al. HtrA1 is a novel mast cell serine protease of mice and men. Mol Immunol 2007;44: 2961-8.
36. Launay S, Maubert E, Lebeurrier N, et al. HtrA1-dependent proteolysis of TGF-β controls both neuronal maturation and developmental survival. Cell Death Differ 2008;15:1408-16.
37. Zacchigna L, Vecchione C, Notte A, et al. Emilin1 links TGF-β maturation to blood pressure homeostasis. Cell 2006; 124:929-42.
38. Dewan A, Liu M, Hartman S, et al. HTRA1 promoter polymorphism in wet age-related macular degeneration. Science 2006;314:989-92.
39. Yang Z, Camp NJ, Sun H, et al. A variant of the HTRA1 gene increases susceptibility to age-related macular degeneration. Science 2006;314:992-3.

Self-Contained Induction of Neurons from Human Embryonic Stem Cells

Tsuyoshi Okuno[1,2], Takashi Nakayama[3], Nae Konishi[1], Hideo Michibata[1], Koji Wakimoto[1], Yutaka Suzuki[1], Shinji Nito[1], Toshio Inaba[2], Imaharu Nakano[4], Shin-ichi Muramatsu[4], Makoto Takano[5], Yasushi Kondo[1]*, Nobuo Inoue[6]

1 Advanced Medical Research Laboratory, Mitsubishi Tanabe Pharma Corporation, Osaka, Japan, **2** Department of Advanced Pathobiology, Graduate School of Life and Environmental Sciences, Osaka Prefecture University, Osaka, Japan, **3** Department of Biochemistry, Yokohama City University School of Medicine, Yokohama, Japan, **4** Division of Neurology, Department of Medicine, Jichi Medical University, Tochigi, Japan, **5** Department of Physiology, Jichi Medical University, Tochigi, Japan, **6** Laboratory of Regenerative Neurosciences, Graduate School of Human Health Sciences, Tokyo Metropolitan University, Tokyo, Japan

Abstract

Background: Neurons and glial cells can be efficiently induced from mouse embryonic stem (ES) cells in a conditioned medium collected from rat primary-cultured astrocytes (P-ACM). However, the use of rodent primary cells for clinical applications may be hampered by limited supply and risk of contamination with xeno-proteins.

Methodology/Principal Findings: We have developed an alternative method for unimpeded production of human neurons under xeno-free conditions. Initially, neural stem cells in sphere-like clusters were induced from human ES (hES) cells after being cultured in P-ACM under free-floating conditions. The resultant neural stem cells could circumferentially proliferate under subsequent adhesive culture, and selectively differentiate into neurons or astrocytes by changing the medium to P-ACM or G5, respectively. These hES cell-derived neurons and astrocytes could procure functions similar to those of primary cells. Interestingly, a conditioned medium obtained from the hES cell-derived astrocytes (ES-ACM) could successfully be used to substitute P-ACM for induction of neurons. Neurons made by this method could survive in mice brain after xeno-transplantation.

Conclusion/Significance: By inducing astrocytes from hES cells in a chemically defined medium, we could produce human neurons without the use of P-ACM. This self-serving method provides an unlimited source of human neural cells and may facilitate clinical applications of hES cells for neurological diseases.

Citation: Okuno T, Nakayama T, Konishi N, Michibata H, Wakimoto K, et al. (2009) Self-Contained Induction of Neurons from Human Embryonic Stem Cells. PLoS ONE 4(7): e6318. doi:10.1371/journal.pone.0006318

Editor: Tailoi Chan-Ling, University of Sydney, Australia

Received June 3, 2008; **Accepted** June 24, 2009; **Published** July 21, 2009

Funding: Part of this work was supported by grants from the Ministry of Education, Science, Sports and Culture, the Japanese Government; and from the Japan Ministry of Health, Labor and Welfare.

Competing Interests: The authors have declared that no competing interests exist.

* E-mail: kondo.yasushi@mc.mt-pharma.co.jp

Introduction

Embryonic stem (ES) cells, derived from the inner cell mass of blastocysts, are pluripotent cells that can differentiate into a variety of cell types including neural cells [1,2]. Among the various basic and clinical applications for ES cells, cell transplantation therapy for central nervous diseases is of particular interest because differentiated neurons do not proliferate, and a relatively large number of donor cells are necessary to replace diseased neurons. Several methods have been developed to prepare neural cells from ES cells. Neurons can be obtained indirectly from ES cells via ectodermal cells in embryoid bodies, which are formed from dissociated ES cells, either by induction with retinoic acid or selection [3,4]. Alternatively, neural stem cells and neurons can be directly differentiated from ES cells without forming embryoid bodies by culturing ES cells on mouse-cultured stroma cells (PA-6) [5], or under chemically defined low-density culture conditions [6]. All of these procedures, however, are time consuming and require highly complicated processes to generate many neurons. In addition, their practicality is limited by the possible teratogenicity caused by culture factors, such as retinoic acid, of differentiated cells. We have previously reported an efficient method to prepare transplantable neural cells from mouse ES cells using a conditioned medium collected from rat primary-cultured astrocytes (P-ACM) [7–9]. In this study, we applied this method to human ES (hES) cells for induction of neurons and astrocytes. Once the astrocytes were derived from hES cells, they could be substituted for primary astrocytes that induce neurons, thus achieving xeno-free production of neurons.

Results

Neural cell differentiation from hES

Four hES cell-lines stably expressing humanized renilla green fluorescent protein (hrGFP) were obtained. These hES cell-lines were kept in undifferentiated state with positive stem cell markers, such as alkaline phosphatase, Oct-4, and SSEA-4. When cultured

in P-ACM containing fibroblast growth factor-2 (FGF-2) under free-floating conditions, colonies of undifferentiated hES cells gave rise to floating spheres composed of neural stem cells and undifferentiated cells, which gradually increased in size during the culture. After 12 days of culture, the spheres were plated onto a poly-L-Lysine/Laminin coated dish and cultivated in neural stem cell medium (NSCM) containing high concentrations of FGF-2 and epidermal growth factor (EGF). Within 24 h, the spheres attached onto the substrate and formed circular clusters of cells. Many of these cells subsequently migrated to the surrounding areas and covered the growth surface of the dish in circular monolayers. After replacing NSCM by P-ACM and culture for 14 days, the spheres differentiated into neurons (Figures 1A, B) and few astrocytes (Figures 1C). These were identified by the neuronal marker tubulin β III isoform (Tuj1) and the astrocytic marker glial fibrillary acidic protein (GFAP).

Selective differentiation of hES cells into neurons and astrocytes

By culture of the spheres in NSCM, neural stem cells were able to migrate from the attached spheres to the surrounding area and subsequently form a circular cluster. NSCM containing FGF-2 and EGF promotes neural stem cells proliferation, while repressing their differentiation into any type of neural cells. After removing the core of the attached spheres mechanically, the remaining neural stem cells could proliferate in NSCM and selectively differentiate into neurons and astrocytes by subculture in an appropriate medium. To differentiate into neurons, neural stem cells were subcultured using 0.05% Trypsin/EDTA in P-ACM for 14 days (Figures 2A, B). After these 14 days of subculture, a large number of cells expressed Tuj1 ($84.0 \pm 5.1\%$, $n = 3$). On the other hand, to differentiate into astrocytes, neural stem cells were subcultured in G5 medium for 14 days (Figure 2C). After this subculture, a large number of cells expressed

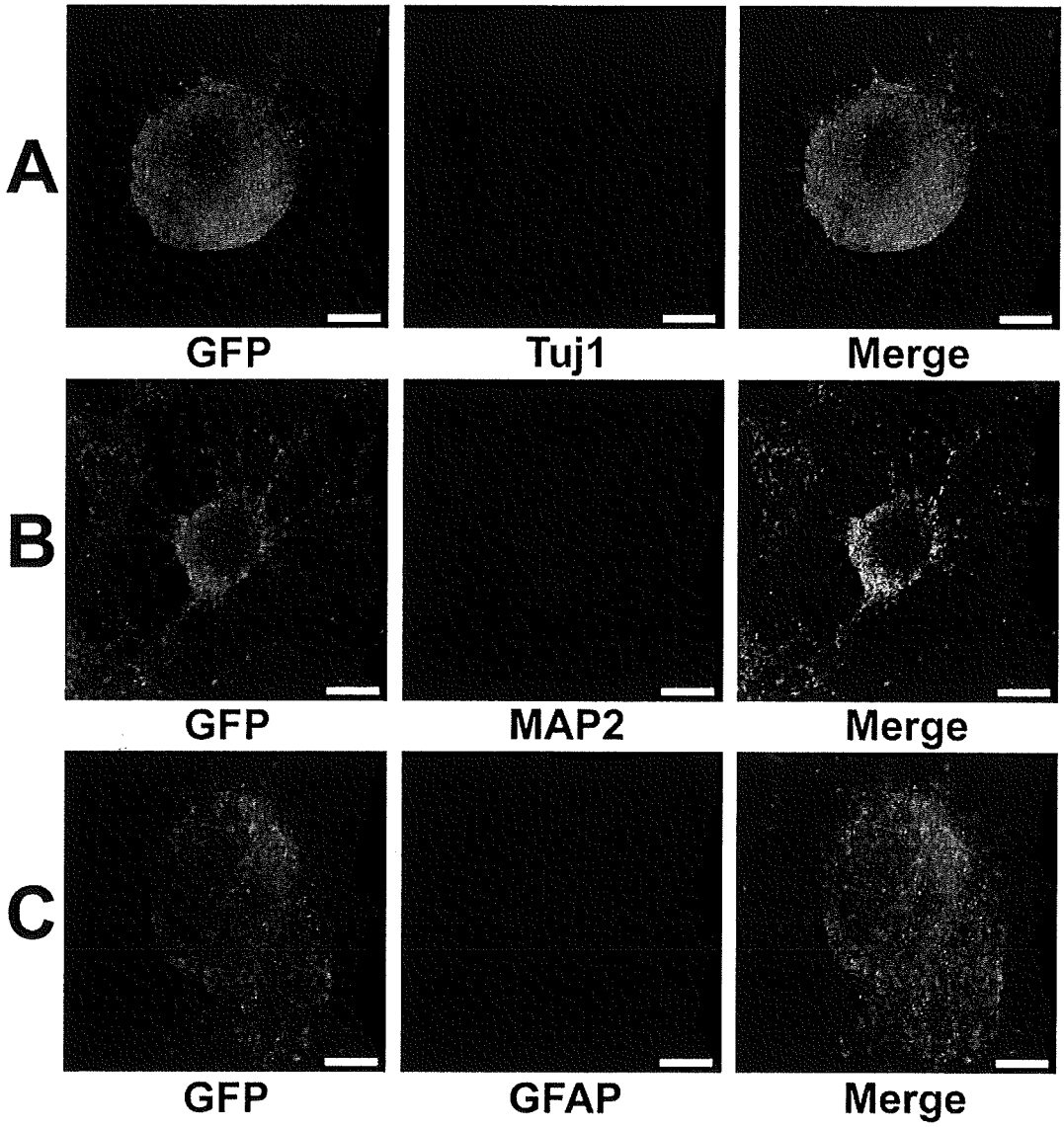

Figure 1. Differentiation of hES cells into neurons in P-ACM. Floating spheres composed of neural stem cells and undifferentiated cells grown for 12 days were plated on an adhesive substrate and cultured for 14 days in P-ACM. Expression of hrGFP (green), Tuj1 (A, red), MAP2 (B, red), and GFAP (C, red) staining of the many neural and few glial cells derived from hES cells. Bar = 100 μm.
doi:10.1371/journal.pone.0006318.g001

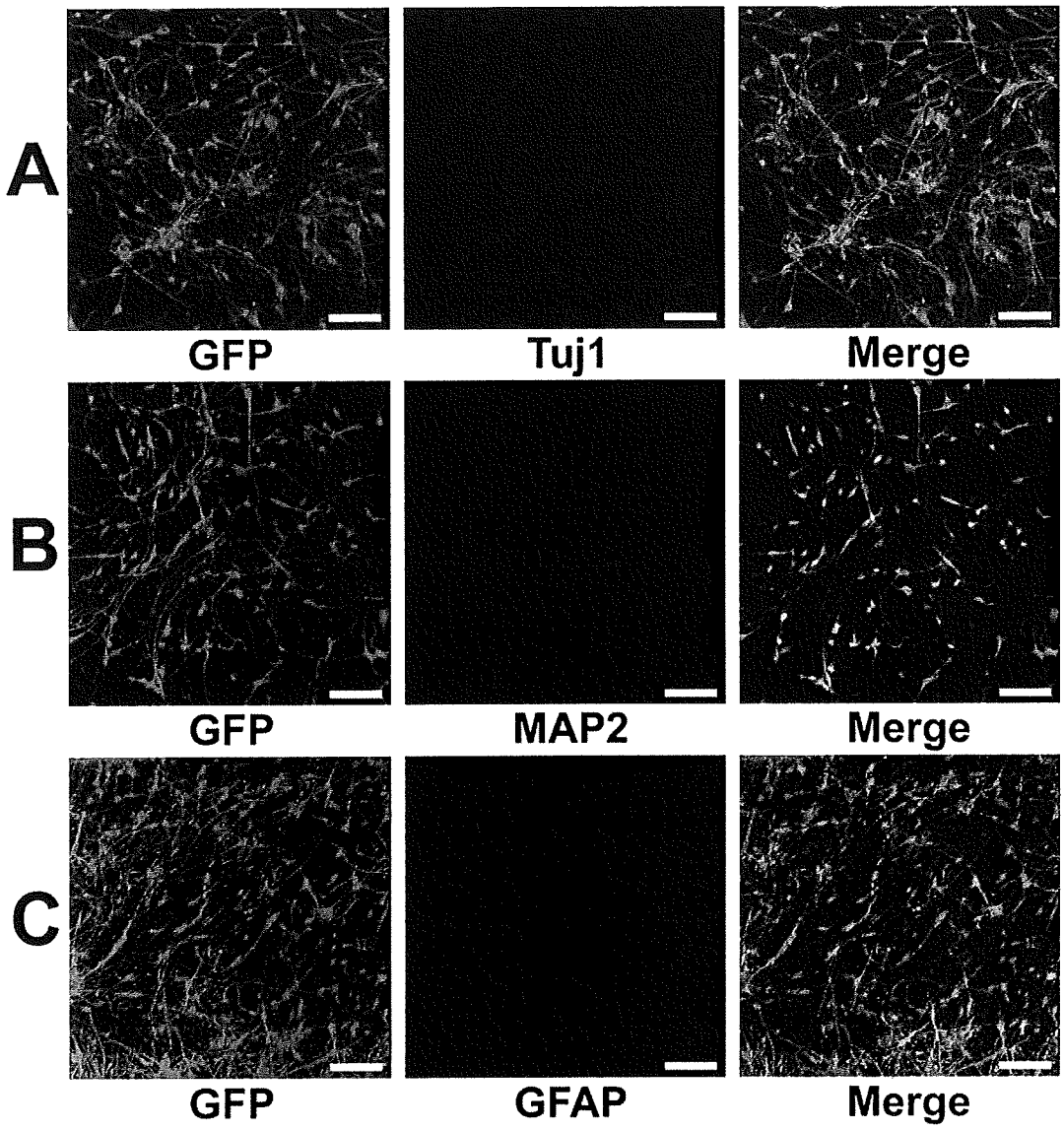

Figure 2. Selective induction of hES cells into neurons and astrocytes. (A, B): Neural stem cells that had migrated from floating spheres in NSCM were subcultured onto a PLL coated plate and cultured for 14 days in P-ACM. Immunostaining with antibody to Tuj1 and MAP2 showed that the subcultured neural stem cells had differentiated into neurons. Expression of hrGFP (green), (A) Tuj1 (red), and (B) MAP2 (red) staining profiles. (C): Neural stem cells were cultured for 14 days after removal of the core of spheres with a glass pipette and change of medium to G5 medium. The proliferated cells were subcultured onto PLL/LAM coated plate and cultured for 14 days in G5 medium. Immunostaining with antibody to GFAP showed that the subcultured cells had differentiated into astrocytes. Expression of hrGFP (green) and GFAP (red) staining profiles. Bar = 100 μm.
doi:10.1371/journal.pone.0006318.g002

GFAP (75.0±1.2%, $n=3$). The removed core of the attached spheres could, like the first spheres, be used repeatedly (about twenty times) as seed for neural stem cells.

Xeno-free induction of astrocytes using a chemically defined medium

For collection of xeno-free astrocytes derived from hES cells, we used a chemically defined N2 medium for neural induction. When cultured in N2 medium containing FGF-2 and EGF under free-floating conditions, colonies of undifferentiated hES cells gave rise to floating spheres. As N2 was less efficient than P-ACM for obtaining astrocytes, we prepared hES cells in large scale ($>10^8$ cells). After differentiation, millions of astrocytes were gained under xeno-free condition (Figure 3A).

Neuronal induction of hES cell-derived astrocytes

Next, we investigated whether the astrocytes derived from hES cells can be substituted for primary astrocytes to differentiate hES cells into neural cells. A conditioned medium of hES cell-derived astrocytes was collected after two days culture and used as ES-ACM by adding an equal amount of N2 medium. As in the case of P-ACM, hES cells cultured in ES-ACM differentiated into neural cells via formation of spheres. After switching the cells from NSCM to ES-ACM, many cells had neuronal-like appearance with long neurites. By 6 weeks of culture in ES-ACM, most cells had neural morphology and expressed microtubule-associated protein 2 (MAP2) (Figure 3B). During our procedure for differentiating hES cells using ES-ACM, expression of several markers was analyzed by RT-PCR (Figure 4A). By 8 weeks culture

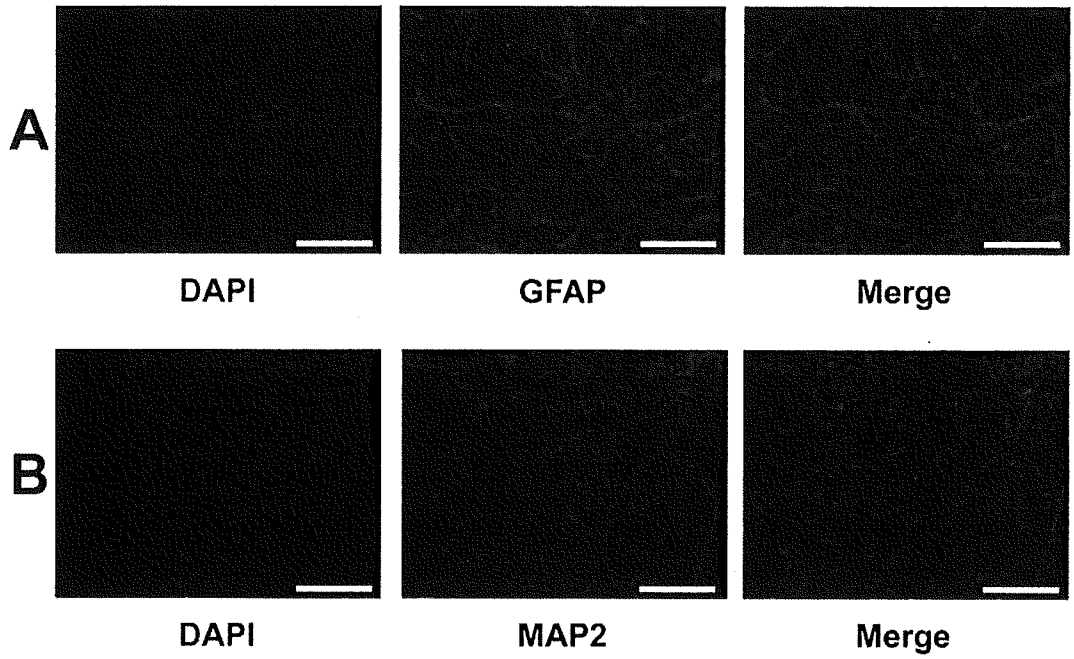

Figure 3. Differentiation of hES cells into astrocytes in a chemically defined medium. (A): Neural stem cells induced by N2 medium were cultured for 14 days after removal of the core of spheres with a glass pipette and change of medium to G5 medium. The proliferated cells were subcultured onto a PLL/LAM coated plate and cultured for 14 days in G5 medium. Immunostaining with antibody to GFAP showed that most of the subcultured cells had differentiated into astrocytes. DAPI (blue) and GFAP (green) staining profiles. Neural stem cells induced by xeno-free ES-ACM were subcultured onto PLL coated plate and cultured for 6 weeks in ES-ACM. (B): Immunostaining with antibody to MAP2 showed that the subcultured NSCs had differentiated into mature neurons. DAPI (blue) and MAP2 (red) staining profiles. Bar = 100 μm.
doi:10.1371/journal.pone.0006318.g003

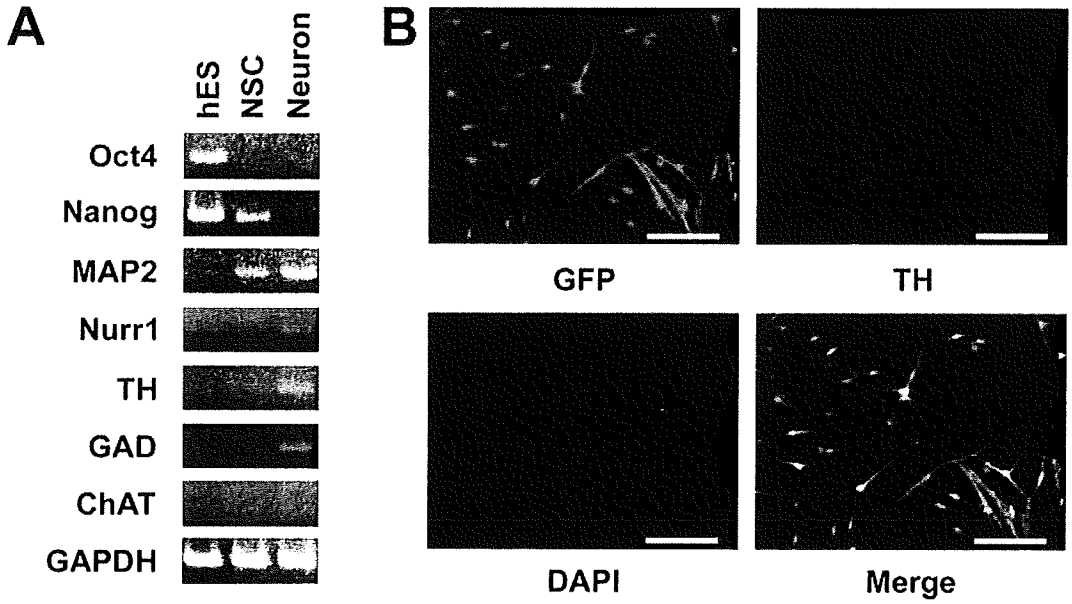

Figure 4. RT-PCR analysis and differentiation of hES cells into dopaminergic neurons in xeno-free ES-ACM. (A): RT-PCR analysis of hES cells, neural stem cells and mature neurons. RNA was isolated from clones of undifferentiated hES cells, from neural stem cells, and from mature neurons which had been cultured for 8 weeks in ES-ACM and analyzed for expression of marker genes. The expression levels of each gene were normalized to GAPDH gene expression level. hES, undifferentiated hES cells; NSC, neural stem cells; Neuron; mature neurons. (B): Differentiation of hES cells into dopaminergic neural cells in xeno-free ES-ACM. Neural stem cells induced by ES-ACM were subcultured onto PLL coated plate and cultured for 8 weeks in ES-ACM. Immunostaining with antibody TH and expression of hrGFP showed that the subcultured neural stem cells had differentiated into dopaminergic neurons. Expression of hrGFP (green), DAPI (blue) and TH (red) staining profiles. Bar = 100 μm.
doi:10.1371/journal.pone.0006318.g004

in ES-ACM, some cells showed tyrosine hydroxylase (TH) -immunoreactivity (Figure 4B). Furthermore, when cultured in ES-ACM again, the cells could differentiate into astrocytes via formation of spheres. To induce differentiation of neural stem cells into astrocytes, the culture medium was changed from NSCM to G5 medium. After medium change, most neural stem cells had the appearance of typical astrocytes. By 2 weeks culture in G5 medium, the majority (82.4±1.8%, $n=3$) of cells expressed GFAP, and few (<1%) expressed MAP2.

Electrophysiological analysis of neurons differentiated from hES cells

For electrophysiological study, hES-derived neurons were cultured on coverslips for 4–6 weeks. The coverslips were transferred to a recording chamber before use. Neurons were selected based on their appearance (spherical shape with long neurites). The resting membrane potential of the neurons were −62.0∼−11.1 mV ($n=26$). Among 26 cells examined, action potentials were elicited in 22 cells (Figure 5A, Control). Application of 1 μM tetrodotoxin (TTX) completely suppressed the overshoot (Figure 5A, right panel). The action potentials were evoked only when resting membrane potentials were set to −70 mV by current injection in 11 cells. The rest of the cells did not possess membrane excitability ($n=4$ out of 26, closed circle in Figure 5B).

Survival of hES cell-derived neurons in mice brain

To examine differentiation of hES cell-derived cells *in vivo*, we transplanted neural stem cells induced with ES-ACM into mice brain ($n=7$). Before transplantation, the majority (85.1±5.1%, $n=4$) of donor cells expressed Nestin, a marker for neural stem cell (Figure 6A), and no cells expressed octamer transcription factor-3 (Oct-3) and stage-specific embryonic antigen (SSEA-4), two makers for undifferentiated cells (data not shown). Four weeks after engraftment, many ($2–3\times10^2$) hrGFP-positive cells were recognized (Figure 6B, C). Some of these cells (<10%) were also Tuj1-immunoreactive (Figure 6D). In the vicinity of the grafts, few cells were immunoreactive against Ki-67, a marker for proliferation. However, none of these Ki-67-positive cells were positive for hrGFP (Figure 6E). Teratoma was not detected in any of the transplanted mice.

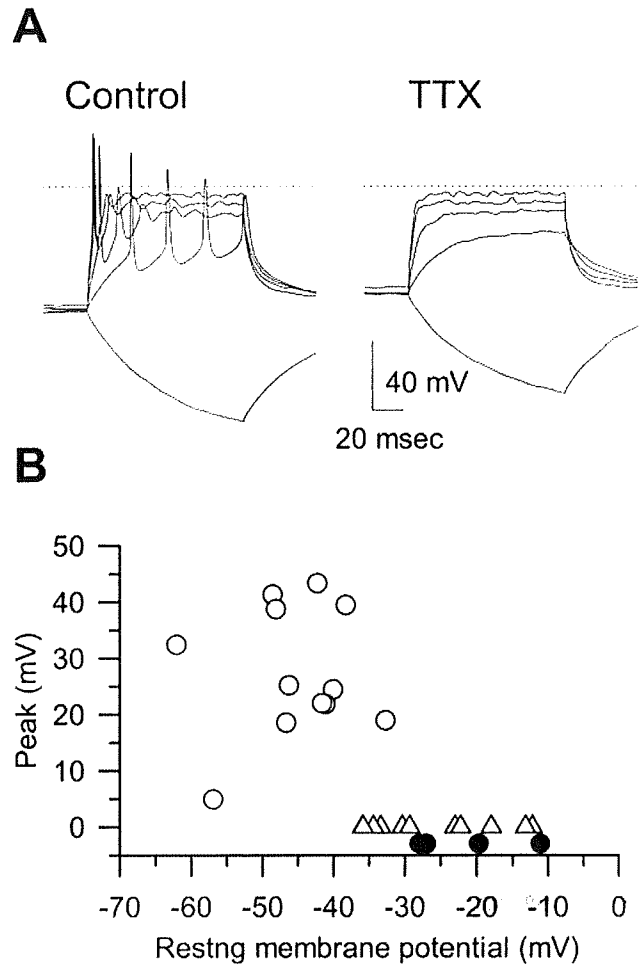

Figure 5. Electrophysiological properties of hES-derived neurons. (A): (Control) Action potentials elicited by depolarizing current injections (50 pA steps for 100 msec). The resting membrane potential was −62.0 mV. During the hyperpolarizing pulse (−50 pA), no 'sug' component was observed. (TTX) Membrane potentials recorded in the presence of 1 μM tetrodotoxin. In both panels, the dotted lines indicate 0 mV. (B): Summary of the resting membrane potentials and the peak amplitudes. Open circle; cells with action potentials. Open triangle; cells with action potentials only when the resting membrane potential was set to −70 mV. Closed circle; cells without membrane excitability.
doi:10.1371/journal.pone.0006318.g005

Discussion

We have shown in this study that neurons and astrocytes can be produced efficiently from hES cells using a conditioned medium collected from either rat primary-cultured astrocytes or hES cell-derived astrocytes. Astrocytes derived from hES cells can be used for continuous generation of neurons. Although a number of media including serum-free media supplemented with various cytokines and/or growth factors have been developed [10,11] to keep a long-term culture of neuronal cells, synthetic culture systems can usually maintain neural cells stable for only few weeks. Although a conditioned medium of primary-cultured astrocytes can be effective in culturing neurons for a longer period of time, the use of primary astrocytes may not be practical due to a number of limitations, including restricted availability of neural tissues as source of astrocytes, and extensive time and effort to obtain astrocytes from living tissues. Additionally, it is very difficult to maintain a stable culture of primary cells in a culture vessel, and subculture of these cells is limited within few passages.

The properties of primary-cultured astrocytes vary depending on the maturation stage of the living body and the region of the living tissue from which the astrocytes are derived. In addition, when astrocytes are obtained from a living body, contamination with cells other than the desired astrocytes is inevitable. Thus, it is difficult to prepare a stable astrocyte-conditioned medium having substantially uniform quality. With our method, on the other hand, ES-ACM can efficiently induce differentiation of hES cells into neural cells. Moreover, large amounts of ES-ACM can be produced stably and readily. ES-ACM, like P-ACM, can keep neuron cultures stable for more than eight weeks until mature neuronal phenotypes are apparent. In addition, completely xeno-free ES-ACM can be generated from immature hES cells by culture in chemically defined medium. With this completely xeno-free ES-ACM, xeno-free neurons and astrocytes can repeatedly be produced. In our transplantation experiment, donor cells did not express undifferentiated markers, such as Oct-3 and SSEA-4. In addition, only few Ki-67 positive cells found in the vicinity of the grafts were hrGFP-negative. These cells were unlikely to be derived from donor cells. It is important to exclude tumorigenicity of neuronal cells derived with this xeno-free method in future

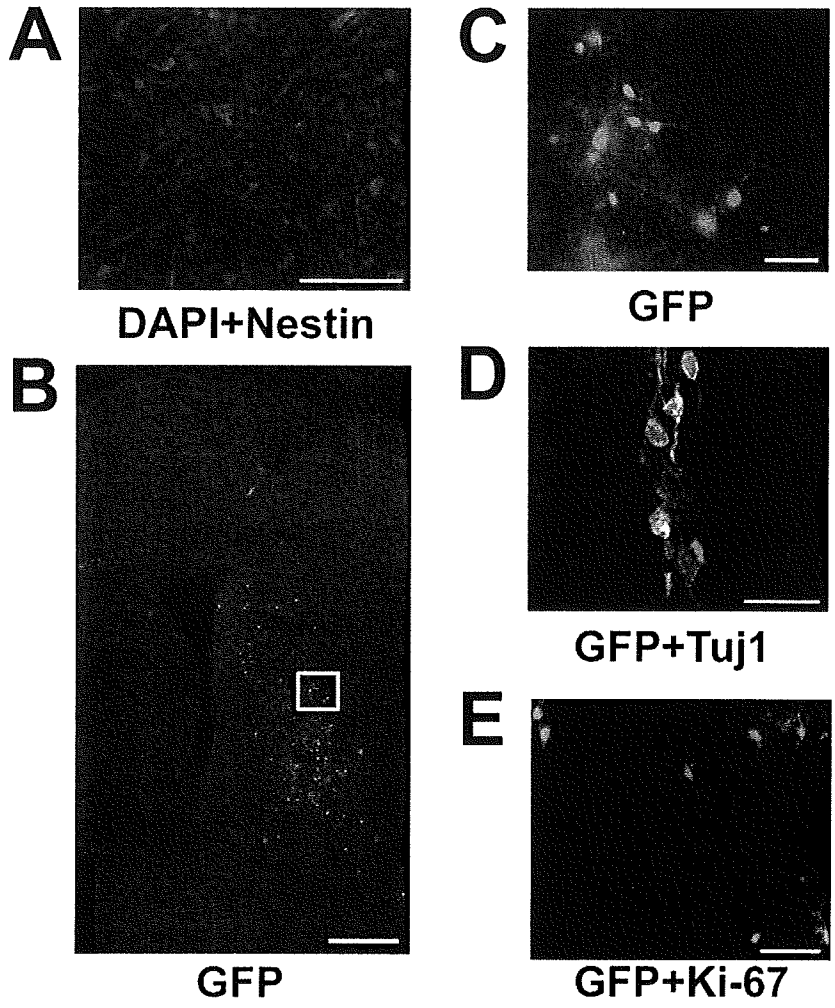

Figure 6. Survival of transplanted neural stem cells *in vivo*. (A): Most of the donor cells were confirmed to be Nestin-immunoreactve neural stem cells before transplantation. Anti-Nestin staining (green) and DAPI (blue). Bar = 50 μm. (B): Transplantation site. Grafted cells expressing hrGFP can be seen in the striatum. Bar = 500 μm. (C): High power magnification view of a white box in panel A. Some of the hrGFP-positive cells display a morphology similar to that of neurons. Bar = 50 μm. (D): Merged image of hrGFP expression (green) and immunostaining of anti-Tuj1 (red). Bar = 20 μm. (E): Merged image of hrGFP expression (green) and immunostaining of anti-Ki-67 (red). Bar = 50 μm.
doi:10.1371/journal.pone.0006318.g006

study for application to the cell therapy. Further studies are necessary to identify the specific molecules that induce neural cells in P- and ES-ACMs.

Recently, two methods adopting human tissue-derived cells have been reported as appropriate for clinical applications. One is an improved stromal cell-induced method that uses an amniotic membrane matrix [12]. The other uses telomerase-immortalized midbrain astrocytes [13]. Although both methods are xeno-free, they still need primary human tissues. On the other hand, with our method, neural cells can be induced from ES cells themselves. This self-serving method can supply donor cells consistently and may have an advantage for clinical applications.

Materials and Methods

ES cell culture

All experiments using hES cells were performed in conformity with "The Guidelines for Derivation and Utilization of Human Embryonic Stem Cells" of the Japanese government after approval by the institutional review board of Mitsubishi Tanabe Pharma Corporation. Two hES cell lines, SA002 and SA181, were obtained from Cellartis AB (Goteborg, Sweden) [14] and maintained on a mitotically inactivated mouse embryonic fibroblast feeder layer in a culture medium (vitroHES, Vitrolife AB, Goteborg, Sweden), supplemented with 4 ng/ml FGF-2 (Invitrogen, Carlsbad, CA). For passaging, the hES cells were treated with collagenase type IV (200 U/ml; Invitrogen) for 5 min, gently scraped from the culture dish, and then split 1:2–1:4 onto a feeder layer of mouse embryonic fibroblasts inactivated with 10 μg/ml mitomycin C.

Electroporation

All recombinant DNA experiments conformed to National Institute of Health (NIH) guidelines. First, a pGFP plasmid, in which hrGFP (Stratagene, La Jolla, CA) was expressed under the control of a CAG promoter (a gift from J. Miyazaki) [15] was constructed. Ten micrograms of the linearized plasmid was then electroporated into a suspension of hES cells (10^7 cells) in 0.8 mL of PBS using a Gene Pulser (500 μF, 250 V, Bio-Rad, Hercules, CA). The cells were next incubated on ice for 10 minutes, plated, and allowed to recover for 24 hours before selection with G418 (200 μg/mL). The cells were daily fed with the culture medium containing G418 for 12 days, after which the resulting ten G418-

resistant ES colonies showing strong hrGFP expression were individually picked and propagated. To analyze stem cell markers, alkaline phosphatase activity and cell surface markers were detected using an ES cell characterization kit (Chemicon, Temecula).

hES cell differentiation

Whole colonies of undifferentiated hES cells, 800–1000 μm in diameter, were picked up from the feeder layer using a glass capillary and transferred into non-adhesive bacteriological dishes each containing P-ACM supplemented with 20 ng/ml FGF-2 (R&D Systems Inc., Minneapolis). P-ACM was prepared as described previously [7]. The colonies were then cultured for 12 days, giving rise to spheres, which were next plated onto poly-L-Lysine/Laminin (Sigma-Aldrich, St. Louis) coated dishes and cultivated for seven days in NSCM (Neurobasal medium supplied with B27 supplement, both from Invitrogen, 20 ng/ml FGF-2, and 20 ng/ml recombinant EGF [R&D systems]). At this stage, the spheres gave rise to circular clusters of cells, many of which migrated from the clusters to the surrounding areas. After replacing the NSCM with P-ACM and culture for 14 days, the spheres differentiated into neurons and few astrocytes. To obtain more and purer neurons, the centers of the clusters containing undifferentiated ES cells were removed with a glass capillary, and the rest of the clusters were cultured for seven days in NSCM. Neuronal differentiation was then induced by subculture of neural stem cells using 0.05% Trypsin/EDTA in P-ACM for 14 days. To induce astrocytic differentiation, the neural stem cells were subcultured in G5 medium (Neurobasal medium supplemented with G5 supplement, both from Invitrogen, 10 ng/ml FGF-2, and 20 ng/ml EGF) for 14 days.

To induce astrocytic differentiation under xeno-free conditions, the colonies of hES cells were transferred into non-adhesive bacteriological dishes each containing N2 medium (Neurobasal medium supplied with N2 supplement, Invitrogen) supplemented with 20 ng/ml of FGF-2 and EGF. After the colonies were cultured for 12 days, few of them gave rise to spheres containing neural stem cells, which were subsequently plated onto poly-L-Lysine/Laminin in G5 medium. Centers of the spheres containing undifferentiated hES cells were removed with a glass capillary, and the rest of the clusters were cultured for seven days in G5 medium. By repeating over this cycle eight times, the spheres were purified to obtain pure neural stem cells. These neural stem cells were subcultured in G5 medium for 14 days to induce astrocytes. For collection of ES-ACM, hES cells derived-astrocytes were cultured in N2 medium for two days.

Immunostaining analysis

hES cells cultured in a 24-well plate were fixed in 4% paraformaldehyde in phosphate-buffered saline (PBS). Immunocytochemistry was performed using standard protocols and antibodies directed against Tuj1 (monoclonal 1:1000), MAP2 (monoclonal, 1:1000), GFAP (polyclonal 1:500), Oct-4 (monoclonal 1:500), SSEA-4 (monoclonal 1:400), Nestin (monoclonal 1:1000) (all from Chemicon), and TH (monoclonal, 1:400) (Acris Antibodies, Hiddenhausen, Germany). Alexa Fluor 594-labeled (Molecular Probes, Eugene, OR) and Cy3-labeled (GE healthcare, Uppsala, Sweden) secondary antibodies were used for visualization. 4′, 6-diamidino-2-phenylindole (DAPI, Kirkegaard Perry Laboratories, Gaithersburg) was used for nuclei staining.

Cell density of neural lineages (neurons and astrocytes) was determined by counting the numbers of DAPI, Tuj^+ and $GFAP^+$ cells per field at a magnification of 200 times using an inverted microscope. Five visual fields were randomly selected and counted for each sample. Numbers presented in figures represent the average percentage and SEM of positive cells over DAPI from three samples per each examination.

RT-PCR analysis

Total RNA was extracted from undifferentiated hES cells, neural stem cells, and neuronal cells using QIAshredder (QIAGEN, Hilden, Germany) and RNeasy Plus Mini kit (QIAGEN). Reverse transcription was carried out using random hexamers at 37°C for 60 minutes according to the manufacturer's instruction for First-Strand cDNA Synthesis Kit (GE Healthcare UK Ltd., Buckinghamshire, UK). PCR was carried out for 30 cycles using the specific primer sets. The reaction cycle was set at 95°C for 30 seconds, 55°C for 30 seconds, and 72°C for 30 seconds. The amplified fragments were subjected to electrophoresis in a 2% agarose gel, which was subsequently stained with ethidium bromide and photographed. The primers used are as follows: glyceraldelyde-3-phosphatedehydrogenase (GAPDH), ACCACAGTCCATGCCATCAC and TCCACCACCCTGTTGCTGTA; Oct4, CGTTCTCTTTGGAAAGGTGTTC and ACACTCGGACCACGTCTTTC; Nanog, AAGACAAGGTCCCGGTCAAG and CCTAGTGGTCTGCTGTATTAC; MAP2, CTTTCCGTTCATCTGCCATT and GCATATGCGCTGATTCTTCA; Nurr1, GCTAAACAAAACTTGCATGC and CTCATATCATGTGCCATACTAG; TH, GAGTACACCGCCGAGGAGATTG and GCGGATATACTGGGTGCACTGG; choline acetyltransferase (ChAT), ATGGGGCTGAGGACAGCGAAG and AAGTGTCGCATGCACTGCAGG; glutamic acid decarboxylase (GAD), ATTCTTGAAGCCAAACAG and TAGCTTTTCCCGTCGTTG.

Electrophysiology

The action potential was recorded using current clamp mode of Axopatch200B amplifier and Digidata 1320 interface (Axon, CA, USA). Physiological bathing solution contained (in mM); 140 NaCl, 5.4 KCl, 0.33 NaH_2PO_4, 0.5 $MgCl_2$, 1.8 $CaCl_2$, 5 HEPES (pH = 7.4 with NaOH). Standard high K^+ pipette solution contained; 110 Aspartic acid, 30 KCl, 5 MgATP, 5 Na_2 creatine phosphate, 0.1 Na_2GTP, 2 EGTA, 10 HEPES (pH = 7.2 with KOH). Electrode resistance was 8~6 MOhm. All experiments were carried out at 33–35°C.

Transplantation Experiment

Neural stem cells derived from hES cells using ES-ACM were implanted into the mouse striatum. All animal experimental protocols were approved by the Animal Ethics Committee of Mitsubishi Tanabe Pharma Corporation. 8-week-old C57BL/6 Cr Slc mice (SLC, Shizuoka, Japan) were anesthetized with pentobarbital and fixed on a stereotactic device (Narishige, Tokyo, Japan). By using a glass pipette with an inner diameter of 100 μm, 1×10^5 cells/5 μl were slowly (0.3 μl/min) injected into the striatum (AP±0 mm, ML +2.0 mm, DV −3.0 mm from bregma) of an adult male mouse. Four weeks after the transplantation, the recipient mouse was anesthetized with pentobarbital and perfused with ice-cold 4% paraformaldehyde in PBS. The brains of each mouse were postfixed in the same solution, cryoprotected with 30% sucrose in PBS for 48 h, and frozen. Coronal sections (thickness 40 μm) were cut on a microtome with freezing unit, collected in PBS (pH 7.4), and divided into series. Brain sections were incubated overnight with primary antibodies at 4°C. The primary antibodies used for immunohistochemistry ware mouse anti-Tuj1 (1:800, Covance, USA) and rabbit anti-Ki67 (1:25, abcam, UK). For detection of the primary antibodies, Alexa Fluor 594 goat anti-mouse IgG (1:1000; Molecular Probes) and Alexa

Fluor 594 goat anti-rabbit IgG (1:1000; Molecular Probes) were incubated with the samples. Immunoreactivity was assessed and viewed under confocal laser scanning microscopy (FV10i; Olympus, Tokyo).

Acknowledgements

We thank Jun-ichi Miyazaki, Osaka University Medical School, Osaka, Japan for the generous gift of plasmid pCAG. We also thank Naomi Takino and Hiroko Nishida, Division of Neurology, Department of Medicine, Jichi Medical University, Tochigi, Japan, for their technical assistance.

Author Contributions

Conceived and designed the experiments: TO HM SiM YK. Performed the experiments: TO NK HM KW MT. Analyzed the data: TO HM YS SN TI IN SiM MT YK. Contributed reagents/materials/analysis tools: TN SiM MT NI. Wrote the paper: TO SiM MT YK.

References

1. Thomson JA, Itskovitz-Eldor J, Shapiro SS, Waknitz MA, Swiergiel JJ, et al. (1998) Embryonic stem cell lines derived from human blastocysts. Science 282: 1145–1147.
2. Suemori H, Tada T, Torii R, Hosoi Y, Kobayashi K, et al. (2001) Establishment of embryonic stem cell lines from cynomolgus monkey blastocysts produced by IVF or ICSI. Dev Dyn 222: 273–279.
3. Bain G, Kitchens D, Yao M, Huettner JE, Gottlieb DI (1995) Embryonic stem cells express neuronal properties in vitro. Dev Biol 168: 342–357.
4. Okabe S, Forsberg-Nilsson K, Spiro AC, Segal M, McKay RD (1996) Development of neuronal precursor cells and functional postmitotic neurons from embryonic stem cells in vitro. Mech Dev 59: 89–102.
5. Kawasaki H, Mizuseki K, Nishikawa S, Kaneko S, Kuwana Y, et al. (2000) Induction of midbrain dopaminergic neurons from ES cells by stromal cell-derived inducing activity. Neuron 28: 31–40.
6. Tropepe V, Hitoshi S, Sirard C, Mak TW, Rossant J, et al. (2001) Direct neural fate specification from embryonic stem cells: a primitive mammalian neural stem cell stage acquired through a default mechanism. Neuron 30: 65–78.
7. Nakayama T, Momoki-Soga T, Inoue N (2003) Astrocyte-derived factors instruct differentiation of embryonic stem cells into neurons. Neurosci Res 46: 241–249.
8. Nakayama T, Momoki-Soga T, Yamaguchi K, Inoue N (2004) Efficient production of neural stem cells and neurons from embryonic stem cells. Neuroreport 15: 487–491.
9. Nakayama T, Sai T, Otsu M, Momoki-Soga T, Inoue N (2006) Astrocytogenesis of embryonic stem-cell-derived neural stem cells: Default differentiation. Neuroreport 17: 1519–1523.
10. Bottenstein JE, Sato GH (1979) Growth of a rat neuroblastoma cell line in serum-free supplemented medium. Proc Natl Acad Sci U S A 76: 514–517.
11. Brewer GJ, Cotman CW (1989) Survival and growth of hippocampal neurons in defined medium at low density: advantages of a sandwich culture technique or low oxygen. Brain Res 494: 65–74.
12. Ueno M, Matsumura M, Watanabe K, Nakamura T, Osakada F, et al. (2006) Neural conversion of ES cells by an inductive activity on human amniotic membrane matrix. Proc Natl Acad Sci U S A 103: 9554–9559.
13. Roy NS, Cleren C, Singh SK, Yang L, Beal MF, et al. (2006) Functional engraftment of human ES cell-derived dopaminergic neurons enriched by coculture with telomerase-immortalized midbrain astrocytes. Nat Med 12: 1259–1268.
14. Heins N, Englund MC, Sjoblom C, Dahl U, Tonning A, et al. (2004) Derivation, characterization, and differentiation of human embryonic stem cells. Stem Cells 22: 367–376.
15. Niwa H, Yamamura K, Miyazaki J (1991) Efficient selection for high-expression transfectants with a novel eukaryotic vector. Gene 108: 193–199.

SYNAPSE 63:541–548 (2009)

Multitracer Assessment of Dopamine Function After Transplantation of Embryonic Stem Cell-Derived Neural Stem Cells in a Primate Model of Parkinson's Disease

SHIN-ICHI MURAMATSU,[1]* TSUYOSHI OKUNO,[2] YUTAKA SUZUKI,[2] TAKASHI NAKAYAMA,[3] TAKEHARU KAKIUCHI,[4] NAOMI TAKINO,[1] ASAKO IIDA,[1] FUMIKO ONO,[5] KEIJI TERAO,[5] NOBUO INOUE,[6] IMAHARU NAKANO,[1] YASUSHI KONDO,[2] AND HIDEO TSUKADA[4]

[1]*Divison of Neurology, Department of Medicine, Jichi Medical University, Tochigi 329-0498, Japan*
[2]*Mitsubishi Tanabe Pharma Corporation, Osaka 532-8505, Japan*
[3]*Department of Biochemistry I, Yokohama City University School of Medicine, Kanagawa 236-0004, Japan*
[4]*Central Research Laboratory, Hamamatsu Photonics K.K., Shizuoka 434-8601, Japan*
[5]*Tsukuba Primate Research Center, National Institute of Biomedical Innovation, Ibaraki 305-0843, Japan*
[6]*Division of Regenerative Neurosciences, Tokyo Metropolitan University, Tokyo 116-8551, Japan*

KEY WORDS ES cell; PET; monkey; MPTP

ABSTRACT The ability of primate embryonic stem (ES) cells to differentiate into dopamine (DA)-synthesizing neurons has raised hopes of creating novel cell therapies for Parkinson's disease (PD). As the primary purpose of cell transplantation in PD is restoration of dopaminergic neurotransmission in the striatum, in vivo assessment of DA function after grafting is necessary to achieve better therapeutic effects. A chronic model of PD was produced in two cynomolgus monkeys (M-1 and M-2) by systemic administration of neurotoxin. Neural stem cells (NSCs) derived from cynomolgus ES cells were implanted unilaterally in the putamen. To evaluate DA-specific functions, we used multiple [^{11}C]-labeled positron emission tomography (PET) tracers, including [β-^{11}C]L-3,4-dihydroxyphenylalanine (L-[β-^{11}C]DOPA, DA precursor ligand), [^{11}C]-2β-carbomethoxy-3β-(4-fluorophenyl)tropane ([^{11}C]β-CFT, DA transporter ligand) and [^{11}C]raclopride (D_2 receptor ligand). At 12 weeks after grafting NSCs, PET demonstrated significantly increased uptake of L-[β-^{11}C]DOPA (M-1:41%, M-2:61%) and [^{11}C]β-CFT (M-1:31%, M-2:36%) uptake in the grafted putamen. In addition, methamphetamine challenge in M-2 induced reduced [^{11}C]raclopride binding (16%) in the transplanted putamen, suggesting release of DA. These results show that transplantation of NSCs derived from cynomolgus monkey ES cells can restore DA function in the putamen of a primate model of PD. PET with multitracers is useful for functional studies in developing cell-based therapies against PD. **Synapse 63:541–548, 2009.**

INTRODUCTION

In Parkinson's disease (PD), the cardinal symptoms such as rest tremor, muscular rigidity and bradykinesia, become apparent after 40–50% of the neurons in the substantia nigra pars compacta (SNc) have been lost and striatal dopamine (DA) has been reduced to about 20% of normal levels (Kish et al., 1988). As a treatment for advanced PD, neural transplantation has been investigated for more than two decades with the aim of replacing degenerated DA neurons and restoring dopaminergic neurotransmission in the striatum. Embryonic stem (ES) cells may offer a substitute for currently used fetal midbrain cells, because they can proliferate extensively in an undifferentiated state and may provide an unlimited source of DA neurons (Li et al., 2008; Newman and Bakay, 2008). Transplantation of DA neurons derived from mouse ES cells

Contract grant sponsors: Ministry of Health, Labor and Welfare of Japan, Ministry of Education, Culture, Sports, Science and Technology of Japan (Special Coordination Funds), Japan Society for the Promotion of Science (Grant-in-Aid for Creative Scientific Research), CREST, the Japan Science and Technology Agency (JST).

*Correspondence to: Shin-Ichi Muramatsu, Division of Neurology, Department of Medicine, Jichi Medical University, 3311-1 Yakushiji, Shimotsuke, Tochigi 329-0498, Japan. E-mail: muramats@ms.jichi.ac.jp

Received 18 August 2008; Accepted 31 October 2008

DOI 10.1002/syn.20634

Published online in Wiley InterScience (www.interscience.wiley.com).

showed electrophysiological and behavioral properties expected of neurons from the midbrain in a rat model of PD (Chung et al., 2006; Kim et al., 2002; Rodriguez-Gomez et al., 2007). Survival of DA neurons obtained in vitro from primate ES cells was also reported in primate hosts (Sanchez-Pernaute et al., 2005; Takagi et al., 2005), but the dopaminergic function of these cells in the primate brain has not been fully evaluated.

Positron emission tomography (PET) is a valuable method for imaging altered DA function in PD. The most common tracer used to visualize and assess the integrity of DA presynaptic systems is 6-[^{18}F]fluoro-L-4-dihydroxyphenylalanine ([^{18}F]FDOPA), a fluoro-analog of 4-dihydroxyphenylalanine (L-dopa). However, uptake of this agent is increased in variable conditions such as inflammation and tumor formation, and assessment of graft function using only this ligand is difficult. The present study therefore used PET with multitracers to analyze both presynaptic and postsynaptic dopaminergic functions and found that transplantation of neural stem cells (NSCs) induced from primate ES cells restored DA function in a primate model of PD.

MATERIALS AND METHODS

Cell culture and differentiation

Astrocyte-conditioned medium (ACM) was prepared by culturing astrocytes obtained from mouse fetal cerebra (Inoue et al., 1988) in DMEM/F12 medium (Invitrogen, Carlsbad, CA) containing N2 supplement (Invitrogen). The CMK6 cynomolgus monkey ES cell line (Suemori et al., 2001) was seeded at a clonal density and grown on a mitomycin C-treated mouse embryonic fibroblast feeder layer in DMEM/F12 medium (Invitrogen) supplemented with 1000 U/ml leukemia inhibitory factor (Chemicon, Temecula, CA), 1 mM β-mercaptoethanol (Invitrogen), and 15% knockout serum replacement (Invitrogen). Colonies of undifferentiated ES cells with a diameter of 300–500 μm and grown for 7–9 days were treated with 0.1% collagenase for 5 min and then detached whole using a glass capillary. Colonies were transferred to nonadhesive bacteriological dishes in ACM supplemented with 20 ng/ml of recombinant human fibroblast growth factor (FGF)-2 (R&D Systems, Minneapolis, MN) and 20 ng/ml of recombinant epidermal growth factor (EGF) (R&D Systems). Colonies were cultured for 10 days, giving rise to floating spheres comprising numerous NSCs. To stimulate proliferation, these spheres were plated onto Matrigel-coated dishes and cultivated for up to 10 days in Neurobasal medium (Invitrogen) supplemented with 2% B-27 (Invitrogen), 20 ng/ml of FGF-2, and 20 ng/ml of EGF. To efficiently induce DA-synthesizing neurons, the medium was replaced with ACM supplemented with 50 ng/ml of sonic hedgehog (Shh; R&D Systems) 1 day before transplantation.

Animals and neurotoxin treatment

All experiments were performed in full compliance with the requirements of the institutional animal care and use committee. Two cynomolgus monkeys (*Macaca fascicularis*), M-1 and M-2, weighing 2.3–2.5 kg were used for the cell therapy experiments. The monkeys were housed under standard conditions of humidity and dark/light cycles with ad libitum access to food and water. To create bilateral striatal lesions, 1-methyl-4-phenyl-1,2,3,6-tetrahydropyridine (MPTP, 0.2–0.4 mg/kg of free base; Sigma-Aldrich Japan K.K., Tokyo, Japan) in phosphate-buffered saline (PBS) was injected intravenously once per week over a 4-month period until a stable parkinsonian syndrome was observed. The total dose of MPTP administered was 1.5 and 2.95 mg/kg. To avoid the possibility of spontaneous recovery from the effects of MPTP, which could mimic the behavioral effect of cell transplantation, the monkeys were allowed to recover for 2 months after the last MPTP treatment.

Transplantation procedures

All surgical procedures were performed in an aseptic environment with the monkeys under isoflurane (1–2%) anesthesia. The head was placed in a stereotaxic device (Kopf Instruments, Tujunga, CA). Each monkey received nine injections of NSCs derived from cynomolgus monkey ES cells (M-1, 1×10^5 viable cells; M-2, 2×10^7 viable cells) in three tracts in the left putamen. NSCs were trypsinized and resuspended in 72 μl of ACM supplemented with Shh. Eight microliters of NSC suspension was injected into each of the nine points using a 50-μl Hamilton microsyringe fitted with a 26-gauge needle over a period of 5 min. The needle was left in place for an additional 3 min to prevent the loss of cells by backflow. As a control, 25 μl of ACM supplemented with Shh was injected into the right putamen. Stereotaxic coordinates of injection sites in the putamen were: Track 1, anterior 13.4 mm, lateral 12 mm, depth +19, 17, 15 mm from the midpoint of the ear bar; Track 2, anterior 16.4 mm, lateral 11.5 mm, depth +20, 18, 16 mm; and Track 3, anterior 18.1 mm, lateral 11 mm, depth +19, 17, 15 mm. From 3 days before surgery, the monkeys received daily intramuscular injections of 0.5 mg/kg of the immunosuppressant FK506 (Astellas Pharmaceuticals, Osaka, Japan) diluted in physiological saline. From 5 days after surgery, the dose was reduced to 0.2 mg/kg for the rest of the experimental period.

PET

Magnetic resonance imaging (MRI) of both monkeys was performed at the National Institute for Physiological Sciences using a 3.0-T imager (Allegra; Sie-

mens, Erlangen, Germany) under pentobarbital anesthesia. Stereotaxic coordinates of PET and MRI were adjusted based on the orbitomeatal (OM) plane with a specially designed head holder. Syntheses of [^{11}C]-labeled-compounds have been described (Tsukada et al., 2000a,b). Data were collected on a high-resolution animal PET scanner (SHR-7700; Hamamatsu Photonics, Hamamatsu, Japan) with a transaxial resolution of 2.6 mm full-width at half-maximum and a center-to-center distance of 3.6 mm (Watanabe et al., 1997). The PET camera allowed 31 slices to be recorded simultaneously. After fasting overnight, the monkey under isoflurane anesthesia was secured to a monkey head folder with stereotaxic coordinates aligned parallel to the OM plane. Each of the [^{11}C]-labeled compounds was delivered through a posterior tibial vein cannula. PET with [^{11}C]L-3,4-dihydroxyphenylalanine (L-[β-^{11}C]DOPA), the precursor of DA synthesis, and [^{11}C]raclopride, a reversible D_2 receptor antagonist, were performed for a total of 64 min with 6 time frames at 10 sec intervals and 12 time frames at 1 min, followed by 16 time frames at 3 min. PET with [^{11}C]2β-carbomethoxy-3β-(4-fluorophenyl)-tropane ([^{11}C]β-CFT) was performed with an additional 19 time frames at 3 min for a total of 91 min. To measure DA release in the striatum indirectly in vivo as reflected by reductions in DA receptor availability, [^{11}C]raclopride was injected through the cannula 30 min after administration of either 0.5 mg/kg of amphetamine or saline. Time-activity curves of each labeled compound in regions of interest chosen from magnetic resonance images were obtained.

For quantification of in vivo binding of [^{11}C]raclopride and [^{11}C]β-CFT, a kinetic 3-compartment analysis method was applied as previously described (Huang et al., 1986). The time-activity curves of plasma and of each region were fitted to a 3-compartment model using the least-squares method. Binding potentials of [^{11}C]raclopride and [^{11}C]β-CFT were calculated by determining the ratio of the estimated k_3 value (association rate) to the estimated k_4 value (dissociation rate). For quantification of L-[β-^{11}C]DOPA utilization rate constant in the striatum of the monkey brain, a graphical analysis method was applied to calculate DA synthesis rate (k_3) as described previously (Tsukada et al., 2000a,b).

Behavioral assessment

Animals were clinically evaluated twice a week using a primate parkinsonism rating scale (PPRS) and activities were recorded on digital videotape. The PPRS is based on the Unified Parkinson's Disease Rating Scale, but was developed specifically for nonhuman primates (Jenner, 2000). On PPRS, scores from 0 (normal) to 4 (maximal disability) are given for each of the six following parkinsonian features: spatial hypokinesia in movements around the cage, bradykinesia, manual dexterity of the right arm, manual dexterity of the left arm, balance, and freezing.

Immunocyto- and immunohistochemistry

Cells cultured on coverslips were fixed with 4% paraformaldehyde in 0.1 M PBS (pH 7.2) for 20 min at 4°C. Cells were then treated with 10% normal horse serum, 2% bovine albumin, and 0.2% Triton X-100 in 0.1 M PBS (pH 7.2) for 20 min at room temperature and incubated further in the presence of the following antibodies separately: nestin (1:200, Chemicon); high-molecular-mass neurofilament protein (NF-H) (1:500, Chemicon); glial fibrillary acidic protein (GFAP) (1:200, Chemicon); O4 (1:200, Chemicon); tyrosine hydroxylase (TH) (1:500, Chemicon); aromatic L-amino acid decarboxylase (AADC) (1:200, Sigma); DA transporter (DAT) (1:200, Chemicon); choline acetyl transferase (ChAT) (1:500 Chemicon); serotonin (5HT) (1:1000, Sigma); and glutamic acid decarboxylase (GAD) (1:1000, Sigma). Cells were washed and then incubated in Alexa Fluor 488- and Alexa Fluor 594-labeled secondary antibodies (1:200; Molecular Probes, Eugene, OR). Cells were mounted in Vectashield containing 4,6-diamidino-2-phenylindole (DAPI; Vector Laboratories, Burlingame, CA) and analyzed under a fluorescence microscope (Eclipse E800; Nikon, Tokyo, Japan) equipped with phase-contrast optics or under a confocal laser-scanning microscope (LSM 510; Carl Zeiss Microimaging Co., Tokyo, Japan). Quantitative immunocytochemical data obtained from 4 to 9 cultures are expressed as mean ± standard error of the mean.

Under deep anesthesia, monkeys were perfused with 4% paraformaldehyde through the ascending aorta. The brains were removed and cut into several blocks 5-mm thick. These blocks were postfixed in the same fixative, left for 3 days in PBS containing 30% sucrose, and then cut on a cryostat into coronal sections 30-μm thick. Sections were treated with 0.3% H_2O_2 for 15 min to inhibit endogenous peroxidase. Sections were incubated at 4°C for 2 days in PBS containing 0.3% Triton X-100 and primary antibodies against mouse monoclonal anti-TH antibody (1:8000; Immnostar, Hudson, WI). Next, sections were incubated in biotinylated antimouse immunoglobulin (Ig)G (1:1000; Vector Laboratories) for 1 h at room temperature, and finally in avidin-biotin-peroxidase complex (1:50; Vector Laboratories) for 30 min at room temperature. Peroxidase activity was revealed in 50 mM Tris-HCl buffer (pH 7.6) containing 0.0004% H_2O_2 and 0.01% 3,3′-diaminobenzidine-4HCl (DAB) (all from Vector Laboratories). For immunofluorescence staining, sections were incubated with mouse monoclonal anti-TH antibody (1:800; Immnostar), rabbit anti-5HT antibody (1:2500; Incstar,

Stillwater, MN), or anti-Ki 67 antibody (1:200; Chemicon) followed by incubation with Alexa Fluor 594-conjugated goat antimouse IgG (1:1000; Molecular Probes). Immunoreactivity was assessed and viewed under confocal laser scanning microscopy (TCS NT; Leica Microsystems, Tokyo, Japan). We estimated TH-immunoreactive (IR) cell counts in serial sections (every 10th) under ×63 magnification on a Zeiss microscope equipped with a video camera.

RESULTS

Efficient induction of DA neurons in culture

A colony of undifferentiated ES cells formed spheres with unique concentric stratiform structure when cultivated in ACM supplemented with FGF-2 and EGF under free-floating conditions, as reported previously (Nakayama et al., 2003, 2004). These spheres displayed peripheral NSCs with a center of proliferating ES cells. Subsequent culture on an adhesive substrate formed circular clusters of cells from which many nestin-positive NSCs migrated. After a few passages, almost all cells expressed nestin (99.5% ± 0.5%) and only a few cells (<0.5%) expressed NF-H. To examine differentiation properties in vitro, a small fraction of NSCs were grown in ACM with Shh. After 5 days, cells in culture displayed a neuronal appearance with long neuritis and became positive for NF-H (99.5% ± 0.5%). Cells were immunoreactive for neither antibody against the astrocyte marker GFAP nor the antibody against oligodendrocyte protein O4 (data not shown). Moreover, many (70% ± 1%) NF-H-positive cells expressed DA neuronal markers such as TH, AADC, and DAT (Fig. 1). Small proportions of NF-H-positive cells expressed either 5HT (12.2% ± 1.3%), ChAT (1.0% ± 0.6%), or GAD (11.9% ± 1.6%).

DA production is restored in the grafted putamen

We used PET to assess nigrostriatal dopaminergic function in MPTP-treated monkeys before and after NSC implantation. MPTP-intoxicated monkeys displayed comprehensive loss of uptake for L-[β-^{11}C]DOPA, a substrate for AADC, and [^{11}C]β-CFT, a DA transporter ligand, in both hemispheres of the brain before transplantation, suggesting severe loss of DA terminals (Figs. 2A and 2B). At 4 weeks postoperatively, we found increases in both L-[β-^{11}C]DOPA and [^{11}C]β-CFT uptake in the grafted putamen. Quantitative analysis of scans at 4 weeks after implantation revealed significant increases in both L-[β-^{11}C]DOPA uptake (M-1, 41%; M-2, 61%) and [^{11}C]β-CFT uptake (M-1, 33%; M-2, 36%) in the implanted striatum compared with the control putamen (Figs. 2C and 2D). The degree of decrease in striatal radioactivity from [^{11}C]raclopride after amphetamine challenge in M-2 was significantly higher in the grafted putamen (16%) than in the control putamen (0.6%), indicating increased release of DA in the striatum (Fig. 3).

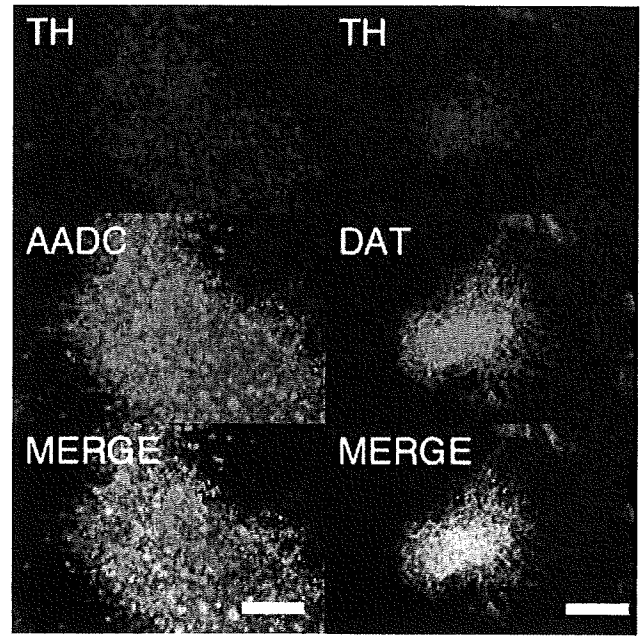

Fig. 1. Neurons derived from ES cells show markers of DA-synthesizing cells. Dual labeling with antityrosine hydroxylase (TH) and antiaromatic L-amino acid decarboxylase (AADC) antibodies shows coexpression of dopamine (DA)-synthesizing enzymes in the neurons. Dual labeling with anti-TH and anti-DA transporter (DAT) antibodies indicates the DA phenotype. Scale bar: 50 μm.

Behavioral recovery is modest

After chronic administration of MPTP, monkeys developed bilateral parkinsonism manifested by a loss of spontaneous motor activity, bradykinesia, impairment of manual dexterity, tremor, and freezing. Parkinsonian features were stable for 2 months from the last MPTP treatment. Three months after unilateral cell transplantation into the putamen, both monkeys showed modest behavioral improvements demonstrated by both PPRS and systematic analysis of digital videotapes. Before MPTP treatment, both monkeys scored 0 on PPRS. After MPTP, but before implantation, mean scores of four evaluations on the PPRS were 14 for M-1 and 12 for M-2. At 12 weeks after implantation, this score reduced to 11 and 10, respectively. In M-2, the score remained constant during the observation period until 6 months after implantation. Regardless of on- or off-medication, no dyskinesia was observed.

Grafted cells differentiate into TH-positive cells in the brain

Histological assessment of brains was performed for M-1 and M-2 at 3 and 6 months after implantation,

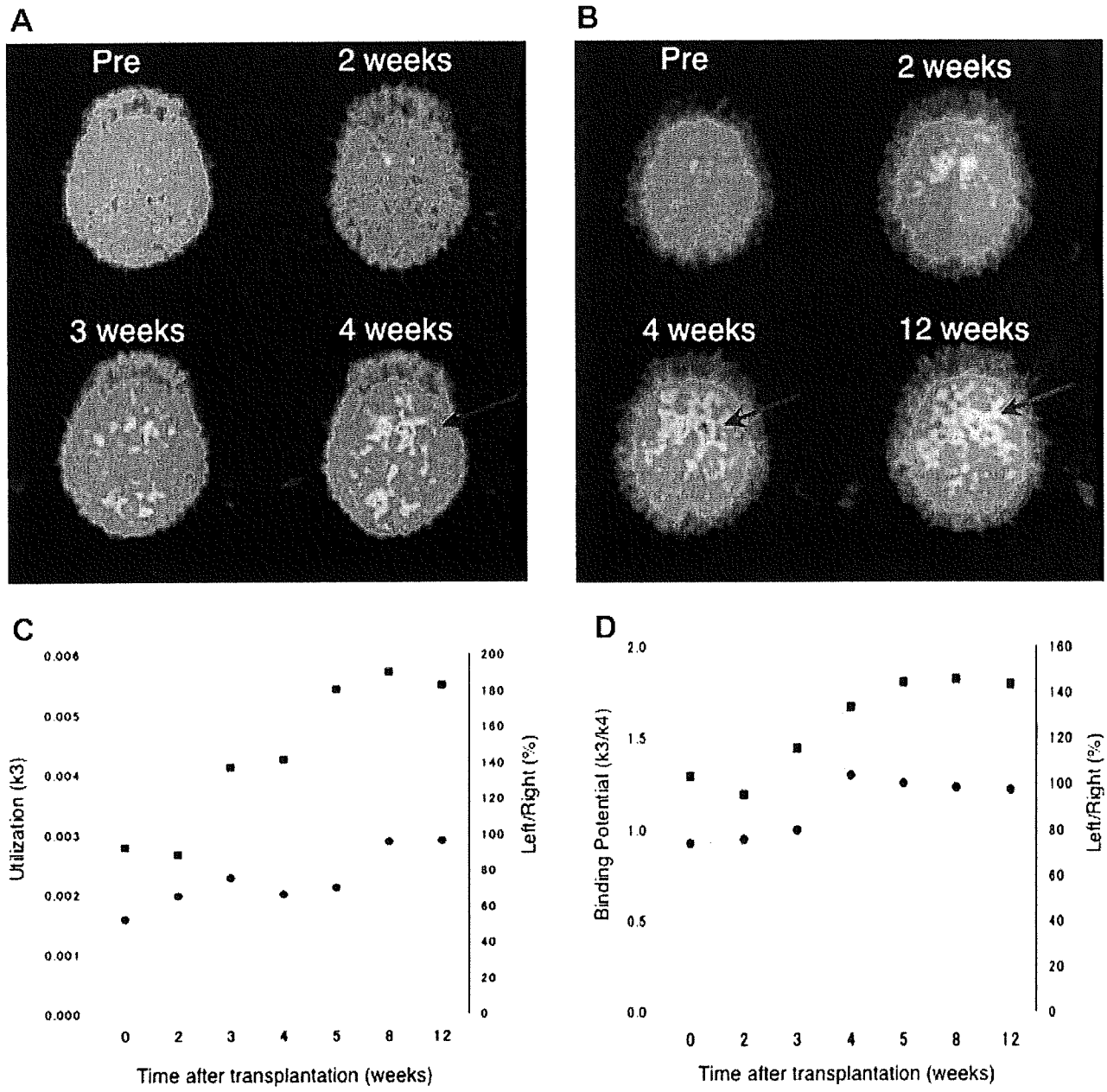

Fig. 2. (**A**, **B**) PET images of L-[β-^{11}C]DOPA (A) and [^{11}C]β-CFT (B) uptake in monkey M-1 before and after cell transplantation. Four weeks after implantation, increased radionuclide uptake was detected in the implanted putamen (arrows). (**C**, **D**) Graphic representation of relative changes in signal strength over time in the same animal, showing significant increases in L-[β-^{11}C]DOPA utilization (k_3 value) (C) and [^{11}C]β-CFT binding potential (BP) (k_3/k_4 value) (D) in the implanted (left: open circles) putamen compared with control (right: filled circles) putamen. Filled squares indicate left to right ratio.

respectively. Many TH-IR cells, about 1000 in M-1 and 3000 in M-2, thrived in the grafted putamen (Fig. 4). Less than 50 TH-IR cells were found in the putamen on the side contralateral to the graft. A small number of 5HT-IR cells was identified in the grafted putamen (<5 cells). No TH-positive cells were positive for the proliferation marker Ki-67. Hematoxylin and eosin staining showed no signs of teratoma-like structures in the transplanted putamen.

DISCUSSION

This study demonstrated with PET that engraftment of NSCs derived from primate ES cells has the capacity to restore DA function in a primate model of PD. Transplantation of neural precursors has become one of the key strategies for cell replacement in the brain. To bypass the shortage of donor tissue, a wide range of experimental approaches have been studied, including proliferation of NSCs in vitro stimulated by

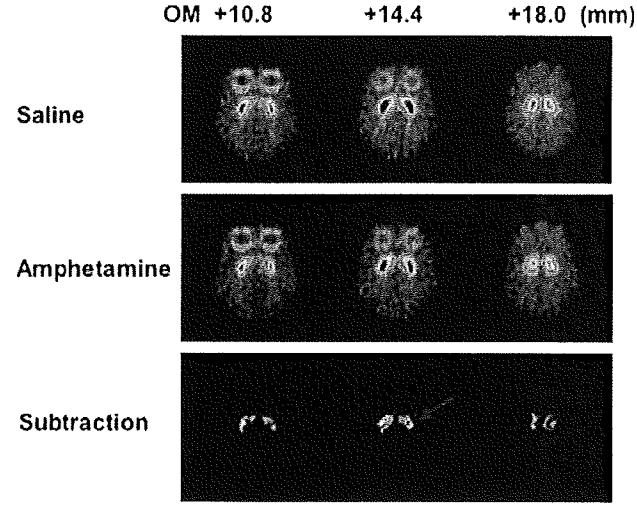

Fig. 3. Drug-induced release of DA in the grafted striatum 12 weeks after transplantation in monkey M-2. After methamphetamine administration, [^{11}C]raclopride binding in the implanted putamen was significantly reduced compared with that in the control putamen. Each slice image after methamphetamine infusion (middle row) was subtracted from a corresponding baseline image (upper row). Subtraction images (lower row). The images of each column are in horizontal plane and same stereotaxic coordinates (mm) from the orbitomeatal (OM) line. Arrows indicate the side of the implant.

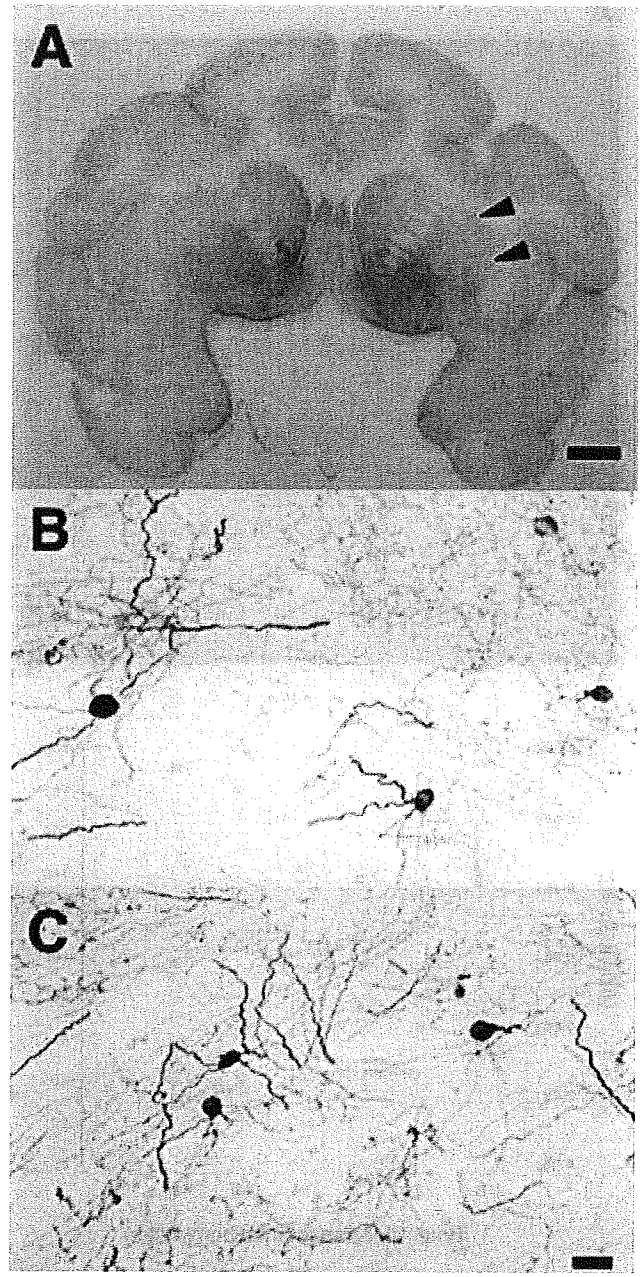

Fig. 4. TH-IR cells in the unilateral putamen of monkey M-1 at 3 months after cell implantation. (**A**) Restoration of TH-IR in the implanted putamen (arrowhead) is not obvious at low magnification. However, TH-IR neurons are apparent in dorsal (**B**) and ventral (**C**) portions of the implanted putamen. Scale bar: 0.5 cm (A); 20 μm (B, C).

mitogen treatment, ex vivo introduction of growth stimulating oncogenes, xenotransplantation, enhancement of endogenous adult neurogenesis, and attempts to recruit non-neural adult stem cells from other tissues (Hall et al., 2007; Liu, 2008). However, in addition to the limited plasticity and slow propagation of adult stem cells, continuous expression of oncogenes or stimulation of mitogens raises question about the long-term safety of these strategies. Of the various candidate donor cells, ES cells are the most attractive due to the characteristics of pluripotency and the potential for unlimited self-renewal. Although human ES cells seem promising for clinical applications, an alternative model system based on ES cells derived from nonhuman primates is necessary for preclinical studies, including allogenic transplantation.

The present study used cynomolgus monkey ES cells that resemble human ES cells but are distinct from murine ES cells in terms of morphology, expression of surface markers and feeder- and leukemia inhibitory factor-dependence, among other factors (Suemori et al., 2001). We have previously shown that astrocyte-derived factors instruct mouse and primate ES cells to differentiate into neurons quickly and efficiently (Nakayama et al., 2003, 2004). This ACM method is superior to previous methods in terms of simplicity, efficiency, and productivity of neural differentiation. The number of cells was increased 1000-fold, along with differentiation from ES cells into NSCs. NSCs can be highly purified without using either magnetic- or fluorescence-activated cell sorting, and incorporation of undifferentiated ES cells is virtually eliminated. Although low doses of undifferentiated mouse ES cells transplanted into rat striatum developed into fully differentiated DA neurons (Bjorklund et al., 2002), elimination of undifferentiated ES cells is crucial for reducing the risk of tumor formation. Consistent with our previous observations,

culture of NSCs derived from cynomolgus monkey ES cells on an adhesive substrate in ACM exclusively promoted differentiation into neurons.

Parkinsonian features were induced by intravenous administration of MPTP over a period of several months. MPTP causes slowly progressive loss of DA neurons in the substantia nigra, resulting in primates showing all the clinical signs of PD, including tremor, rigidity, akinesia, and postural instability (Wichmann and DeLong, 2003). We created bilateral striatal lesions but implanted cells unilaterally, so one side could serve as a control. Functional effects of the graft were evaluated by comparing PET images of the implanted putamen with those of the contralateral putamen. PET can be used to assess DA function in vivo (Brooks, 2004) by following increases in L-[β-^{11}C]DOPA uptake or [^{11}C]β-CFT binding, which are attributable to the expression of AADC and storage of DA in the putamen and thus indicate graft survival and development of DA neurons. In addition, functional DA release from the graft was demonstrated by imaging D_2 receptor occupancy. Degrees of decrease in striatal radioactivity of [^{11}C]raclopride after amphetamine challenge were significantly higher in the grafted putamen. Based on microdialysis studies, a 1% change in striatal [^{11}C]raclopride binding has been estimated to correspond to a $\geq$8% change in synaptic DA levels (Breier et al., 1997). We identified numerous TH neurons in the grafted putamen. Although small populations of TH neurons may be found in the primate striatum after creating lesions of the nigrostriatal dopaminergic pathways, most are located in the caudate and precommissural putamen (Mazloom and Smith, 2006). The dramatic increase in the number of TH-IR cells in the postcommissural putamen suggests that these TH-IR cells were derived from the graft and contributed to the restoration of dopaminergic function.

Behavioral recovery was modest at 12 weeks after implantation. More DA neurons and synaptic DA release might be necessary for apparent behavioral recovery. Improving neuronal survival and increasing axonal outgrowth would possibly improve the magnitude of the response to grafting. In this regard, the combination of cell replacement and neuroprotective strategies by gene delivery may be effective in preventing the loss of endogenous and grafted NSCs. Another possible explanation for incomplete behavioral recovery is that functional integration of DA neurons with the host circuitry may take place gradually. PD patients with implanted fetal DA neurons show continuous symptomatic improvements even after DA storage capacity in the striatum (measured by L-[β-^{11}C]DOPA PET) and response to DA-releasing agents has plateaued (Isacson et al., 2001; Piccini et al., 2000). With bilateral implantation, further amelioration of global parkinsonism (including enhanced spontaneous activity and improved balance) would be expected, since only 20% of thalamic projections from the basal ganglia are crossed in monkeys (Parent and Hazrati, 1995) and unilateral implantation would mainly affect contralateral limb movement. Monkeys did not display dyskinesia with or without L-dopa. This result supports previous observations that functional DA grafts do not independently generate abnormal DA responses (Bjorklund et al., 2002).

Given the recent successful isolation of nuclear-transferred ES cell lines (Tabar et al., 2008), our findings of efficient ES cell transplantation, expansion, and differentiation into functional DA neurons in the primate model have implications for ES cells as a donor source for cell therapy against PD.

ACKNOWLEDGMENTS

The authors thank Astellas Pharmaceuticals (Osaka, Japan) for providing FK506.

REFERENCES

Bjorklund LM, Sanchez-Pernaute R, Chung S, Andersson T, Chen IY, McNaught KS, Brownell AL, Jenkins BG, Wahlestedt C, Kim KS, Isacson O. 2002. Embryonic stem cells develop into functional dopaminergic neurons after transplantation in a Parkinson rat model. Proc Natl Acad Sci USA 99:2344–2349.

Breier A, Su TP, Saunders R, Carson RE, Kolachana BS, de Bartolomeis A, Weinberger DR, Weisenfeld N, Malhotra AK, Eckelman WC, Pickar D. 1997. Schizophrenia is associated with elevated amphetamine-induced synaptic dopamine concentrations: Evidence from a novel positron emission tomography method. Proc Natl Acad Sci USA 94:2569–2574.

Brooks DJ. 2004. Positron emission tomography imaging of transplant function. NeuroRx 1:482–491.

Chung S, Shin BS, Hwang M, Lardaro T, Kang UJ, Isacson O, Kim KS. 2006. Neural precursors derived from embryonic stem cells, but not those from fetal ventral mesencephalon, maintain the potential to differentiate into dopaminergic neurons after expansion in vitro. Stem Cells 24:1583–1593.

Hall VJ, Li JY, Brundin P. 2007. Restorative cell therapy for Parkinson's disease: A quest for the perfect cell. Semin Cell Dev Biol 18:859–869.

Huang SC, Barrio JR, Phelps ME. 1986. Neuroreceptor assay with positron emission tomography: Equilibrium versus dynamic approaches. J Cereb Blood Flow Metab 6:515–521.

Inoue N, Matsui H, Tsukui H, Hatanaka H. 1988. The appearance of a highly digitalis-sensitive isoform of Na+,K+-ATPase during maturation in vitro of primary cultured rat cerebral neurons. J Biochem (Tokyo) 104:349–354.

Isacson O, Bjorklund L, Pernaute RS. 2001. Parkinson's disease: Interpretations of transplantation study are erroneous. Nat Neurosci 4:553.

Jenner P. 2000. Factors influencing the onset and persistence of dyskinesia in MPTP-treated primates. Ann Neurol 47 (4 Suppl 1): S90–S99; discussion S99–S104.

Kim JH, Auerbach JM, Rodriguez-Gomez JA, Velasco I, Gavin D, Lumelsky N, Lee SH, Nguyen J, Sanchez-Pernaute R, Bankiewicz K, McKay R. 2002. Dopamine neurons derived from embryonic stem cells function in an animal model of Parkinson's disease. Nature 418:50–56.

Kish SJ, Shannak K, Hornykiewicz O. 1988. Uneven pattern of dopamine loss in the striatum of patients with idiopathic Parkinson's disease. Pathophysiologic and clinical implications. N Engl J Med 318:876–880.

Li JY, Christophersen NS, Hall V, Soulet D, Brundin P. 2008. Critical issues of clinical human embryonic stem cell therapy for brain repair. Trends Neurosci 31:146–153.

Liu SV. 2008. iPS cells: A more critical review. Stem Cells Dev 17:391–397.

Mazloom M, Smith Y. 2006. Synaptic microcircuitry of tyrosine hydroxylase-containing neurons and terminals in the striatum

of 1-methyl-4-phenyl-1,2,3,6-tetrahydropyridine-treated monkeys. J Comp Neurol 495:453–469.
Nakayama T, Momoki-Soga T, Inoue N. 2003. Astrocyte-derived factors instruct differentiation of embryonic stem cells into neurons. Neurosci Res 46:241–249.
Nakayama T, Momoki-Soga T, Yamaguchi K, Inoue N. 2004. Efficient production of neural stem cells and neurons from embryonic stem cells. Neuroreport 15:487–491.
Newman MB, Bakay RA. 2008. Therapeutic potentials of human embryonic stem cells in Parkinson's disease. Neurotherapeutics 5:237–251.
Parent A, Hazrati LN. 1995. Functional anatomy of the basal ganglia. I. The cortico-basal ganglia-thalamo-cortical loop. Brain Res Brain Res Rev 20:91–127.
Piccini P, Lindvall O, Bjorklund A, Brundin P, Hagell P, Ceravolo R, Oertel W, Quinn N, Samuel M, Rehncrona S, Widner H, Brooks DJ. 2000. Delayed recovery of movement-related cortical function in Parkinson's disease after striatal dopaminergic grafts. Ann Neurol 48:689–695.
Rodriguez-Gomez JA, Lu JQ, Velasco I, Rivera S, Zoghbi SS, Liow JS, Musachio JL, Chin FT, Toyama H, Seidel J, Green MV, Thanos PK, Ichise M, Pike VW, Innis RB, McKay RD. 2007. Persistent dopamine functions of neurons derived from embryonic stem cells in a rodent model of Parkinson disease. Stem Cells 25:918–928.
Sanchez-Pernaute R, Studer L, Ferrari D, Perrier A, Lee H, Vinuela A, Isacson O. 2005. Long-term survival of dopamine neurons derived from parthenogenetic primate embryonic stem cells (cyno-1) after transplantation. Stem Cells 23:914–922.
Suemori H, Tada T, Torii R, Hosoi Y, Kobayashi K, Imahie H, Kondo Y, Iritani A, Nakatsuji N. 2001. Establishment of embryonic stem cell lines from cynomolgus monkey blastocysts produced by IVF or ICSI. Dev Dyn 222:273–279.
Tabar V, Tomishima M, Panagiotakos G, Wakayama S, Menon J, Chan B, Mizutani E, Al-Shamy G, Ohta H, Wakayama T, Studer L. 2008. Therapeutic cloning in individual parkinsonian mice. Nat Med 14:379–381.
Takagi Y, Takahashi J, Saiki H, Morizane A, Hayashi T, Kishi Y, Fukuda H, Okamoto Y, Koyanagi M, Ideguchi M, Hayashi H, Imazato T, Kawasaki H, Suemori H, Omachi S, Iida H, Itoh N, Nakatsuji N, Sasai Y, Hashimoto N. 2005. Dopaminergic neurons generated from monkey embryonic stem cells function in a Parkinson primate model. J Clin Invest 115:102–109.
Tsukada H, Harada N, Nishiyama S, Ohba H, Kakiuchi T. 2000a. Cholinergic neuronal modulation alters dopamine D2 receptor availability in vivo by regulating receptor affinity induced by facilitated synaptic dopamine turnover: Positron emission tomography studies with microdialysis in the conscious monkey brain. J Neurosci 20:7067–7073.
Tsukada H, Harada N, Nishiyama S, Ohba H, Sato K, Fukumoto D, Kakiuchi T. 2000b. Ketamine decreased striatal [(11)C]raclopride binding with no alterations in static dopamine concentrations in the striatal extracellular fluid in the monkey brain: Multiparametric PET studies combined with microdialysis analysis. Synapse 37:95–103.
Watanabe M, Okada H, Shimizu K, Omura T, Yoshikawa E, Kosugi T, Mori S, Yamashita T. 1997. A high resolution animal PET scanner using compact PS-PMT detectors. IEEE Trans Nucl Sci 44:1277–1282.
Wichmann T, DeLong MR. 2003. Pathophysiology of Parkinson's disease: The MPTP primate model of the human disorder. Ann N Y Acad Sci 991:199–213.

運動ニューロン疾患

運動ニューロン疾患の分類と疫学

■分類

運動ニューロンには中心前回のBetz(ベッツ)巨細胞に代表される上位運動ニューロン(UMN；一次運動ニューロン)と脳幹運動神経核・脊髄前角に存在する下位運動ニューロン(LMN；二次運動ニューロン)とがある(図9-90)．運動ニューロン疾患とは，この運動ニューロンが優位におかされて臨床的に運動ニューロン症候(表9-58)が主病像を形成する疾患群を指す．

UMNとLMNの両者がおかされる場合は筋萎縮性側索硬化症(ALS)と呼ばれ，UMNのみが選択的におかされると原発性側索硬化症，LMNのみがおかされると脊髄性筋萎縮症と呼ばれる．

運動ニューロンの障害部位による分類のほかに，孤発性か遺伝性かという観点から分類することもある．

■疫学

ALSの発生率は一般に10万人あたり1～2人といわれ，このうち5～15%が家族性と考えられている．家族性ALSのうち，約2割が後述の変異SOD1(superoxide dismutase 1)を有する遺伝性ALSである．

〔中野今治〕

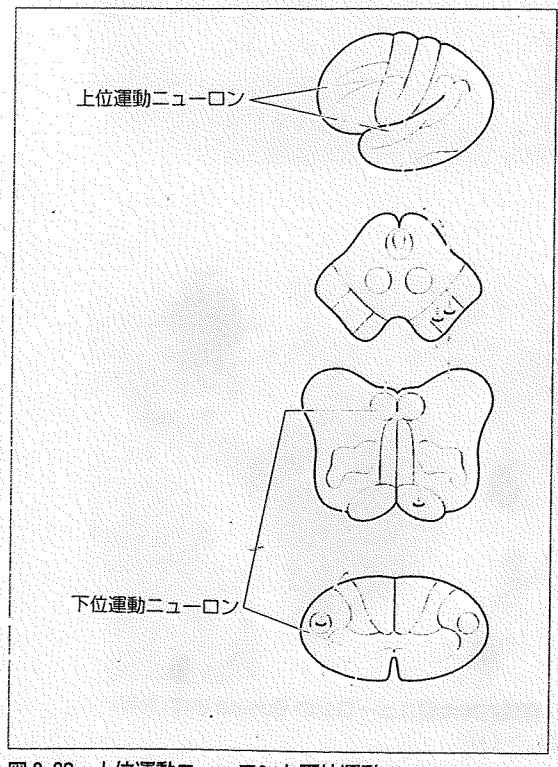

図9-90 上位運動ニューロンと下位運動ニューロン

1 筋萎縮性側索硬化症，家族性筋萎縮性側索硬化症

筋萎縮性側索硬化症(ALS)には孤発性ALSと家族性ALSとがある．前者の代表が古典型〔Charcot(シャルコー)病〕といわれて，孤発性に発症するタイプである．本項ではALSといえば，この古典型を指すことにする．それに対して，家族性ALSは家族発症するタイプであり，その大多数は遺伝性と考えられている．

① 筋萎縮性側索硬化症 amyotrophic lateral sclerosis(ALS)

■概念

UMNとLMNが選択的進行性におかされ，数年で呼吸不全を呈して死亡する運動ニューロン疾患である．

表9-58 神経変性疾患における運動ニューロン症候

症候	障害部位	
	上位運動ニューロン	下位運動ニューロン
筋力低下	軽度	高度
筋萎縮	なし	高度
線維束性収縮	なし	出現
腱反射	亢進	低下～消失
筋緊張	亢進(痙縮，クローヌス)	低下(筋弛緩)
Babinski徴候，Chaddock徴候	陽性	陰性
手指の巧緻運動	軽度障害	高度障害

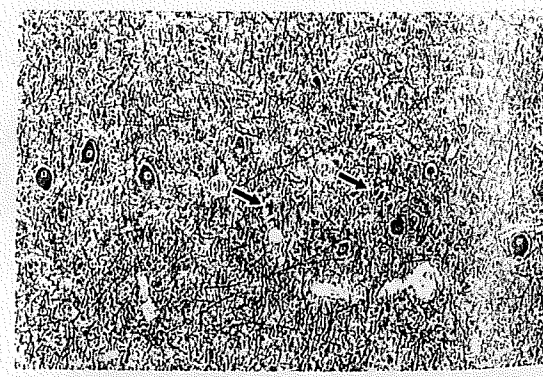

図9-91 筋萎縮性側索硬化症のBetz巨細胞
本例ではよく保存されているようにみえるが，一部は変性(矢印①)，あるいは消失(矢印②)しており，後者では清掃にきたマクロファージが認められる．(KB染色，×100)

■病理・病態生理

ALSの基本的病理は，中心前回のBetz巨細胞に代表される大型ニューロン(図9-91)の脱落，および脳神経運動核の一部(三叉神経運動核，顔面神経核，疑核，副神経核，舌下神経核)と脊髄前角の大型運動ニューロンの脱落である(図9-92)．中心前回ニューロンの脱落とともにその投射路(皮質核路と皮質脊髄路)が変性する．軸索が変性するとそれを取り巻いている髄鞘も崩壊して髄鞘染色〔Klüver-Barrera(KB)染色〕で染まらなくなるので，皮質脊髄路(錐体側索路と錐体前索路)は淡明に見える(図9-93)．

残存しているLMNでは，ほぼ正常に見えるニューロンからさまざまの程度の変性像を呈するニューロンまでが認められる．一部のLMNは好酸性(HE染色で赤く染まること)でしばしば数珠(じゅず)状に連なる円形封入体〔Bunina(ブニナ)小体〕を含んでいる(図9-94)．Bunina小体はALSでのみ出現する重要な構造物である．また，ALSの前角ニューロンにはユビキチン化した封入体(skein-like inclusion と round inclusion)が出現する．この構成成分がTDP-43であることが最近報告された．

運動ニューロン死の機序として酸化ストレス説，ウイルス説，自己免疫説，外毒素説，興奮性アミノ酸(グルタミン酸が代表的)過剰説などが挙げられているが，真の原因は不明である．ALSにおけるLMN死の機序として現在最も注目されているのが，グルタミン酸受容体の1つであるAMPA受容体の分子的変化である．内部に大量のCa^{2+}が流入するとその神経細胞は細胞死に陥る．AMPA受容体はこのCa^{2+}流入を調節しており，その調節に決定的役割を果たすのが受容体のサブユニットの1つであるGluR2である．ALS症例のLMNのGluR2では，元来アルギニンである部位がグルタミンになっており，そのためにCa^{2+}が流入して運動ニューロン死が起こると推測されている．

■臨床所見

◉初発症状

初発症状として最も多いのは，上肢遠位部の筋力低下と筋萎縮である．初期には通常左右のどちらかがおかされる．前腕筋がおかされると握力の低下として現れ，手内筋がおかされると箸がうまく使えない，字がうまく書けないなどの指の巧緻運動障害が出現する．

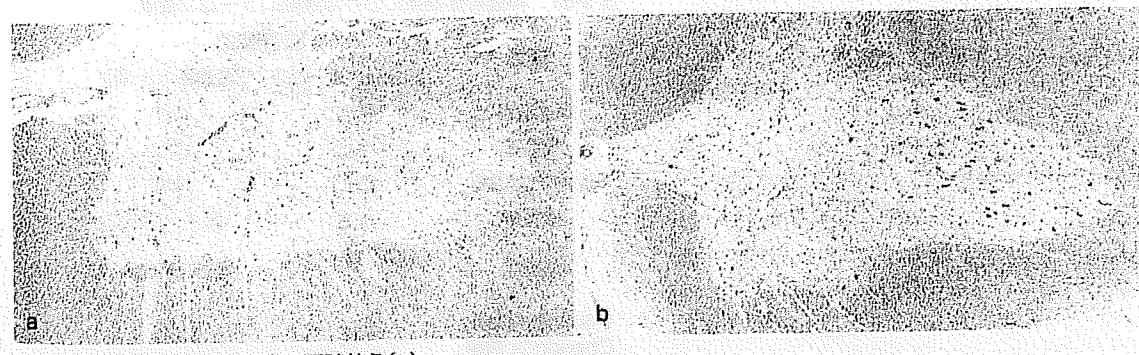

図9-92 筋萎縮性側索硬化症の頸髄前角(a)
対照(b)に比して大型のLMNが高度に脱落している．(KB染色，×40)

図9-93 筋萎縮性側索硬化症の頸髄
錐体側索路(★★)と錐体前索路(★)の淡明化がみられる．(KB染色)

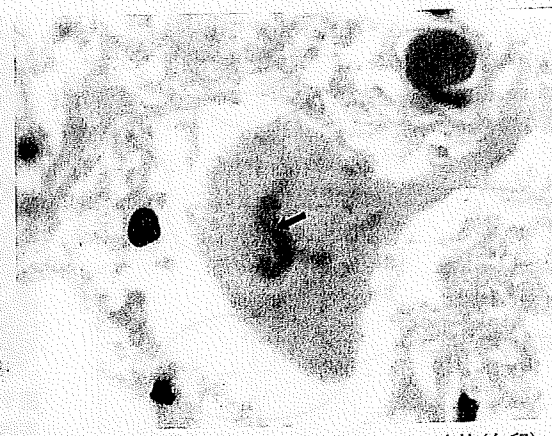

図9-94 脊髄前角大型ニューロンのBunina小体(矢印)
(HE染色，×400)

図 9-95 筋萎縮性側索硬化症の下位運動ニューロン障害による筋萎縮
母指球(a)と舌(b).

2番目に多い初発症状は球麻痺症状であり，なかでも舌筋の運動障害に伴う構音障害が多い．

㋐臨床像

麻痺 いずれの部位から初発しても，筋力低下と筋萎縮は他の部位に徐々に拡大して，球麻痺，四肢麻痺となり数年後には大多数の患者は臥床状態となる．後頸筋群がおかされると頸下がりの状態となり，このときには通常前頸筋群もおかされるので，仰臥位から起き上がるときに頭部を持ち上げられなくなる．

筋萎縮 おかされた筋には筋萎縮と線維束性収縮が認められる．手においては母指球(図 9-95a)と第1背側骨間筋の萎縮が最も同定しやすい．前脛骨筋が萎縮すると，その前縁は脛骨前縁よりも後退するので，前脛骨筋の萎縮も同定しやすい．舌は正常では多少隆起した滑らかな表面を有しているが，萎縮すると凹凸を示すようになる(図 9-95b)．

線維束性収縮 1個の前角運動ニューロンとそれが支配する筋線維群を運動単位といい，1運動単位に属する筋線維の数を神経支配比といい，おおよそ100～数100である．線維束性収縮は，LMNの不随意な興奮によってその運動単位に属する筋線維がすべて同期して収縮する現象であり，数100の筋線維が同時に束として(筋線維束)として収縮することから，肉眼的に観察できる．これに対し，個々の筋線維がばらばらに収縮する線維性収縮は肉眼的には観察できない．線維束性収縮は三角筋や大胸筋などの上肢帯筋，母指球や背側骨間筋，大腿四頭筋の内側頭，オトガイ舌筋でよくみられる．

猿手・鷲手 母指球筋が高度に障害されると母指の対立ができなくなり，手で持つのに第2～5指のみと手掌を使うようになる(猿手；サルは元来母指の対立ができない)．また，中手指節間関節を屈曲し，指節間関節を伸展するのは手内筋である骨間筋と虫様筋である．この筋の筋力低下が生じると中手指節間関節が伸展し，指節間関節の屈曲した状態となる(鷲手)．

球麻痺 舌が萎縮して運動障害が高度になると，発話は遅く不明瞭になる．また，口腔内の食塊を滑らかに咽頭に送り込むことができなくなり，さらには咽頭筋の麻痺により反射性の嚥下運動が障害され，誤嚥をきたすようになる．

呼吸筋麻痺 ALSの進行期に入ると，横隔膜，肋間筋など呼吸筋がおかされ呼吸不全になる．横隔膜が優位におかされたときには，吸気相で腹部が陥凹する奇異性呼吸を示す．

陰性4徴候 ALSでみられない4つの徴候のことをいい，外眼筋麻痺，感覚障害，排尿(便)障害，褥瘡を指す．

㋑検査所見

針筋電図検査 ALSの診断に最も重要な検査である．まず，消失したLMNで支配されていた筋線維群は神経支配を逃れて(脱神経支配)，個々に自発的に収縮するようになる(線維性収縮)．これの電気活動が線維自発電位 fibrillation potential である．ついで，残存したLMNの軸索末端からの発芽 sprouting により，一部の筋線維の再支配が生じるが，新たに形成された側枝の伝導時間は正常より長く，また新しいシナプスでの伝達も不安定であるので，多相性で持続の長い運動単位電位を示す．やがて，再支配が完成してシナプス伝達も安定してくると，1つの運動単位が支配する筋線維の数が増えるので，高振幅，長持続，多相性のいわゆる神経原性変化を示すようになる(図 9-96)．ALSでは，それぞれの運動単位が異なった変性過程にあるので，針筋電図でも脱神経電位(線維自発電位)から高振幅まで種々の運動単位電位を示す．

神経伝導検査 伝導速度の遅延や伝導ブロックはないが，複合筋活動電位の低下がみられる．